



Original article

Anilides and quinolones with nitrogen-bearing substituents from benzothiophene and thienothiophene series: Synthesis, photochemical synthesis, cytostatic evaluation, 3D-derived QSAR analysis and DNA-binding properties



Maja Aleksić^a, Branimir Bertoša^{b,c,**}, Raja Nhili^d, Sabine Depauw^d, Irena Martin-Kleiner^e, Marie-Hélène David-Cordonnier^d, Sanja Tomić^b, Marijeta Kralj^e, Grace Karminski-Zamola^{a,*}

^a Department of Organic Chemistry, Faculty of Chemical Engineering and Technology, University of Zagreb, Marulićev trg 20, P.O. Box 177, HR-10000 Zagreb, Croatia

^b Division of Physical Chemistry, "Ruder Bošković" Institute, Bijenička Cesta 54, P.O. Box 1016, HR-10000 Zagreb, Croatia

^c Division of Physical Chemistry, Faculty of Natural Sciences, University of Zagreb, Horvatovac 102A, HR-10000 Zagreb, Croatia

^d INSERM U837-JPARC (Jean-Pierre Aubert Research Center), Team "Molecular and Cellular Targeting for Cancer Treatment", Université Lille Nord de France, IFR-114, Institut pour la Recherche sur le Cancer de Lille, Place de Verdun, F-59045 Lille Cedex, France

^e Division of Molecular Medicine, "Ruder Bošković" Institute, Bijenička Cesta 54, P.O. Box 1016, HR-10000 Zagreb, Croatia

ARTICLE INFO

Article history:

Received 4 June 2013

Received in revised form

4 November 2013

Accepted 7 November 2013

Available online 15 November 2013

Keywords:

Amides

Quinolones

Antitumor evaluation

QSAR analysis

DNA-binding properties

ABSTRACT

A series of new anilides (**2a–c**, **4–7**, **17a–c**, **18**) and quinolones (**3a–b**, **8a–b**, **9a–b**, **10–15**, **19**) with nitrogen-bearing substituents from benzo[*b*]thiophene and thieno[2,3-*c*]thiophene series are prepared. Benzo[*b*]thieno[2,3-*c*]- and thieno[3',2':4,5]thieno[2,3-*c*]quinolones (**3a–b**, **8a–b**) are synthesized by the reaction of photochemical dehydrohalogenation from corresponding anilides. Anilides and quinolones were tested for the antiproliferative activity. Fused quinolones bearing protonated aminium group, quaternary ammonium group, *N*-methylated and protonated aminium group, amino and protonated amino group (**8a**, **9b**, **10–12**) showed very prominent anticancer activity, whereby the hydrochloride salt of *N,N'*-dimethylaminopropyl-substituted quinolone (**14**) was the most active one, having the IC₅₀ concentration at submicromolar range in accordance with previous QSAR predictions. On the other hand, flexible anilides were among the less active. Chemometric analysis of investigated compounds was performed. 3D-derived QSAR analysis identified solubility, metabolic stability and the possibility of the compound to be ionized at pH 4–8 as molecular properties that are positively correlated with anticancer activity of investigated compounds, while molecular flexibility, polarizability and sum of hydrophobic surface areas were found to be negatively correlated. Anilides **2a–b**, **4–7** and quinolones **3a–b**, **8a–b**, **9b** and **10–14** were evaluated for DNA binding propensities and topoisomerases I/II inhibition as part of their mechanism of action. Among the anilides, only compound **7** presented some DNA binding propensity whereas the quinolones **8b**, **9b** and **10–14** intercalate in the DNA base pairs, compounds **8b**, **9b** and **14** being the most efficient ones. The strongest DNA intercalators, compounds **8b**, **9b** and **14**, were clearly distinguished from the other compounds according to their molecular descriptors by the PCA and PLS analysis.

© 2013 Elsevier Masson SAS. All rights reserved.

1. Introduction

Together with the biological aspects of cancer treatment, chemotherapy using small molecules or bioactive natural products is still the useful manner of cancer treatment, whereby the major cellular targets are DNA and tubulin, along with various protein kinases [1–3]. Therefore, the search for novel small organic molecules with either better activity and/or selectivity is still of great

* Corresponding author. Tel.: +385 14597215; fax: +385 14597250.

** Corresponding author. Division of Physical Chemistry, Faculty of Natural Sciences, University of Zagreb, Horvatovac 102A, HR-10000 Zagreb, Croatia. Tel.: +385 14606132; fax: +385 14606131.

E-mail addresses: bbertosa@irb.hr (B. Bertoša), gzamola@fkit.hr (G. Karminski-Zamola).

importance for developing novel anticancer drugs. Amides and quinolones exhibit several pharmacological activities and have therefore attracted considerable attention from medicinal and synthetic organic chemists [4–7]. Recently some other compounds derived from benzo[*b*]thiophene series showed as potent tubulin polymerization inhibitors [8]. Some similar compounds from benzothienopyran series namely 3-(aryl)benzothieno[2,3-*c*]pyran-1-ones (tricyclic lactones) were prepared by a tandem one-pot Sonogashira coupling and intramolecular cyclization. Tricyclic lactones obtained were evaluated for their capacity to inhibit the *in vitro* growth of three human tumor cell lines, MCF-7 (breast adenocarcinoma), NCI-H460 (non-small cell lung cancer) and SF-268 (CNS cancer). Most of the compounds showed a high growth inhibitory effect on all the tested cell lines, with GI₅₀ values in the μM range. A structure–activity relationship was established for the Sonogashira products and for the tricyclic lactones, namely related to the presence and position of substituents (OMe and/or F) in the benzothienopyran moiety or in the phenyl ring [9]. New organometallic compounds from benzo[*b*]thiophene series with antitumor properties were prepared [10], as well as a series of *N*-(2-(5-fluoro-2-(4-fluorophenylthio)benzo[*b*]thiophen-3-yl)ethyl) acylamides, which were evaluated for their binding affinity and intrinsic activity at melatonin receptors [11]. Also, benzothienopyranes offer interest to pharma industry as scaffolds for synthesis of raloxifene and relevant structural analogues of selective estrogen receptor modulators (SERM) [12].

As a part of our continuing search for potential anticancer agents related to heterocyclic quinolones, we have previously reported synthesis and strong inhibitory activities on several human tumor cell lines of thieno[3',2':4,5]thieno- and benzo[*b*]thieno[2,3-*c*]quinolones, containing a *N,N*-dimethylaminopropyl substituent in the amine part of the molecule and on the quinolone nitrogen [13,14]. Moreover, we also reported the synthesis and antiproliferative activity of various cyano- and/or amidino-substituted benzo[*b*]thieno[2,3-*c*]quinolones and their acyclic precursors [15], since it is well known that amidines are structural parts of numerous compounds of biological interest as various medical and biochemical agents. Amidino-substituted benzo[*b*]thieno[2,3-*c*]quinolones, strong ds-DNA/RNA intercalators, showed in general stronger and more selective antitumor activity than acyclic precursors, which did not intercalate at all. In order to examine impact of thiophene vs. benzene ring, we have also prepared amidino-substituted thieno[3',2':4,5]thieno- and thieno[2',3':4,5]thieno[2,3-*c*]quinolones, as well as their acyclic precursors, whereby both cyclic and acyclic compounds showed pronounced antitumor activity [16]. Replacement of the benzene ring with pyridine, in the amino part of the amides and naphthyridones, and the acyclic amidino groups with cyclic amidino 2-imidazolanyl group, respectively, resulted with increased antitumor activity. Some of the naphthyridone compounds were active in the submicromolar range, with special selectivity to MiaPaCa-2, HeLa and SW620 cells. Compounds with high DNA binding capacity were identified as the most promising inhibitors of tumor growth and of topoisomerase activity whereby the 2-imidazolanyl-substituted derivatives showed the most prominent activity [17].

Further on, a class of substituted benzo[*b*]thienyl- and thieno[2,3-*b*]thienyl-carboxanilides and benzo[*b*]thieno[2,3-*c*]- and thieno[3',2':4,5]thieno[2,3-*c*]quinolones prepared (Fig. 1) in the multistep synthesis and photochemical synthesis was tested for the antiproliferative activity on various tumor cell lines [18]. Using the experimentally obtained antitumor measurements, 3D-derived QSAR models were obtained and molecular properties that have the highest impact on antitumor activity of quinolones were identified. Some of the prepared compounds were evaluated for DNA binding propensities and topoisomerases I and II inhibition as

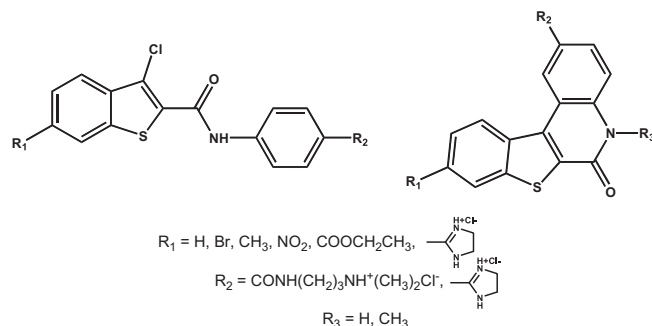


Fig. 1. Earlier prepared benzo[*b*]thienyl-carboxanilides and benzo[*b*]thieno[2,3-*c*]quinolones.

part of their mechanism of action assessment. We have shown that benzo[*b*]thienyl-carboxanilide with 2-imidazolanyl-substituent binds to DNA as a groove binder, while its cyclic analog binds as an intercalator.

Using this knowledge from our previous investigations [18], we synthesized new compounds with a new nitrogen-bearing substituent. Thus, in this work we introduced amino, protonated amino, acetamido, *N,N*-dimethylamino groups, as well as aminium or quaternary ammonium salts in the anilide part of the substituted carboxanilides and quinolones of the benzo[*b*]thiophene and thieno[2,3-*b*]thiophene series. Quinolone nitrogen was in some compounds substituted with methyl or *N,N*-dimethylaminopropyl groups. These changes were made in an attempt to affect properties found by previous QSAR analysis as important for activity, such as, integrity moments and solubility. To elucidate the impact of the variation of thiophene vs. benzene ring, we also prepared nitro, acetamido and *N,N*-dimethylamino substituted thieno[2,3-*b*]thienyl-carboxanilides and thieno[3',2':4,5]thieno[2,3-*c*]quinolone.

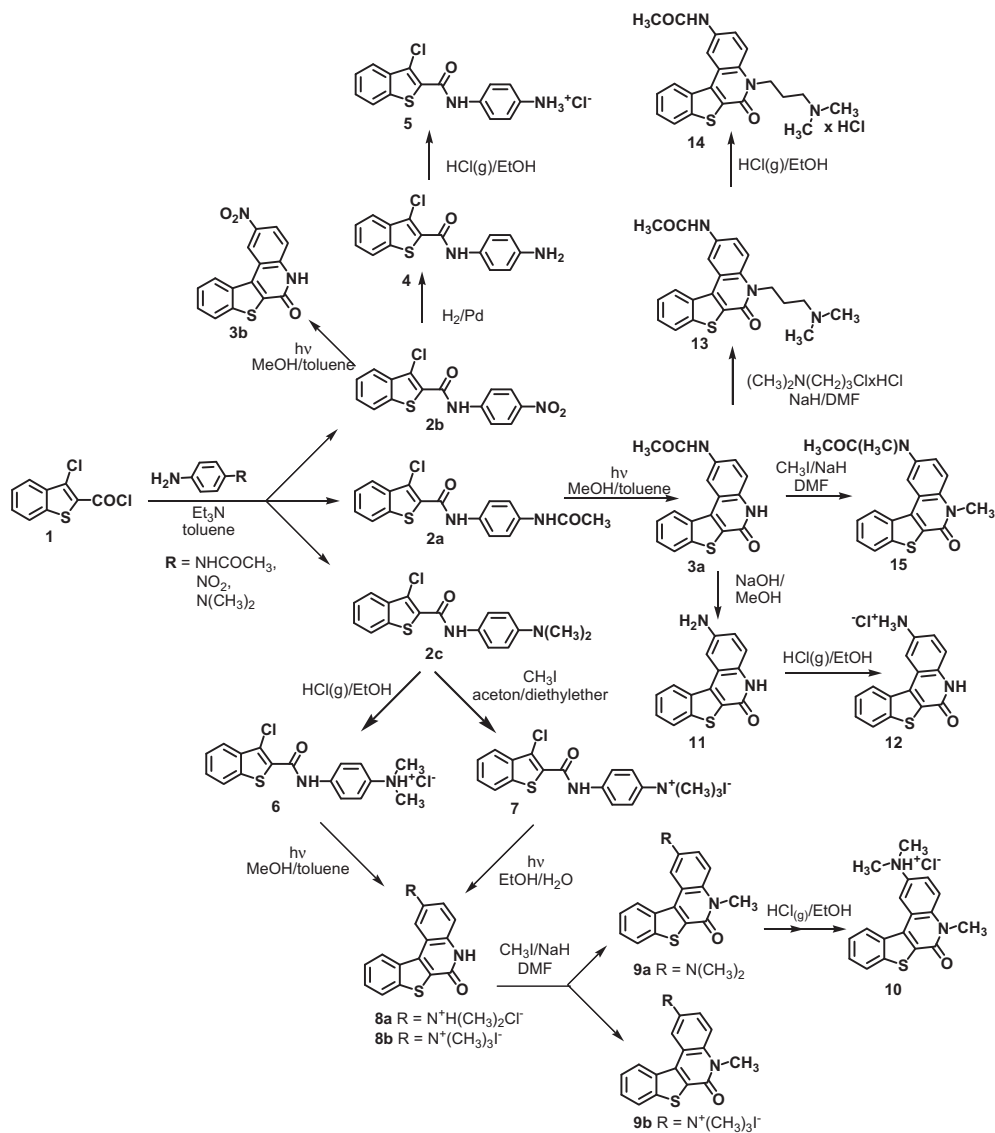
Volsurf [19] based QSAR analysis was applied in order to help us to identify which molecular properties of the studied compounds have the largest impact on antitumor activity. Similar approaches for building 3D-derived QSAR models have already been proven as useful in investigation of different classes of the potentially biologically active compounds [20–24] and can be valuable in designing new compounds with enhanced anticancer activity [24]. Moreover, this paper presents an example of usefulness of the approach in which QSAR analysis serves as a guideline in designing new compounds with increased anticancer activity: the most active compound presented in this paper was designed according to the previous QSAR analysis [25].

2. Results and discussion

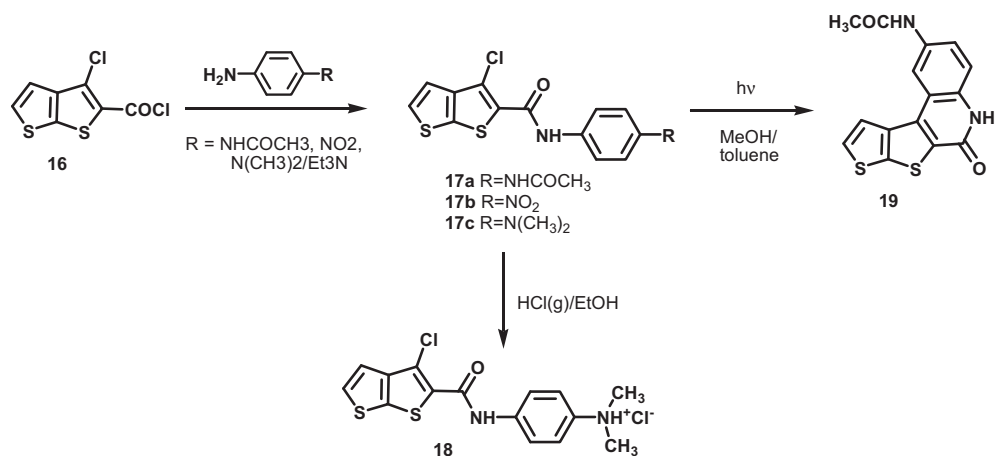
2.1. Chemistry

Prepared compounds were synthesized according to the procedures shown in Schemes 1 and 2 by the conventional methods of organic synthesis for the preparation of similar heterocyclic compounds [13–18].

Starting from the 3-chlorobenzo[*b*]thiophene-2-carbonyl chloride **1** and 3-chlorothieno[2,3-*b*]thiophene-2-carbonyl chloride **16** via condensation reaction with substituted anilines corresponding carboxanilides **2a–c** and **17a–c** were prepared. Carboxanilides **2a–b** were photochemically cyclized into corresponding quinolones **3a–b**. Compound **2b** was also hydrogenated in the presence of palladium into compound **4**. Carboxanilide **2c** was methylated with methyl iodide to obtain quaternary ammonium salt **7**. Quinolone **3a** was hydrolyzed with NaOH into compound **11**. *N*-alkylation of **3a** with *N,N*-dimethylaminopropylchloride hydrochloride in the



Scheme 1. Synthesis of substituted 3-chlorobenzo[b]thiophene-2-carboxamides **2a–c**, **4–7** and benzo[b]thieno[2,3-c]quinolones **8a–b**, **9a–b**, **10–15**.



Scheme 2. Synthesis of 3-chlorothieno[2,3-b]thiophene-2-carboxamides **17a–c**, **18** and thieno[3',2':4.5]thieno[2,3-c]quinolone **19**.

presence of NaH gave the expected quinolone **13**. Carboxanilides **6**, **7** and **17a** were photochemically cyclized into corresponding quinolones **8a**, **8b** and **19**. Quinolones **3a**, **8a–b** were methylated in the presence of NaH in DMF on the lactame nitrogen into *N*-methyl compounds **15**, **9a–b**. During the methylation reaction of compound **8a** the *N,N*-dimethylamino hydrochloride substituent was transformed into the *N,N*-dimethylamino substituent in the **9a** so that the **9a**, without identification, was protonated with HCl_g into aminium salt **10**. Also carboxanilides **2c**, **4**, **17a** and quinolones **11** and **13** were protonated into hydrochloride salts.

Structures of the compounds were confirmed by the ¹H and ¹³C NMR analysis. The formation of the amide bond was supported by the appearance of a one-proton singlet at 9.88 ppm–11.15 ppm in the ¹H NMR spectra of carboxanilides **2a–c**, **4–7**, **17a–c**, **18**. The disappearance of characteristic one-proton singlet of NH quinolone hydrogen at 12.21 ppm–12.59 ppm confirmed that a monoalkylation reaction had taken place for quinolones **3a**, **8a**, and **8b**.

2.2. Antiproliferative activity

Nineteen novel compounds were tested for their potential antiproliferative effect on the three tumor cell lines. In general they exert low to modest effect. However, the majority of the tested compounds were slightly soluble and, besides, the precipitates produced from compound **6**, **2b** and **17b** interfered with the MTT assay, leading to false negative results; therefore these results should be interpreted with caution. In general, quinolones were more active compared to the carboxanilides, but no difference was observed in the activity of their hydrochloride salts. Among carboxanilides compound **7** had the most pronounced effect. The most active compounds, with the IC₅₀ values in the micromolar range, were quinolones **8a**, **9b**, **10**, **11**, **12**, whereby the hydrochloride salt of *N,N*-dimethylamino-propyl-substituted quinolone **14** was the most active one, having the IC₅₀ concentration at submicromolar range (0.2–0.6 μM) (Fig. 2). Compound **14** was designed according to our previous QSAR analysis as compound with potentially high anticancer activity [25]. Experiments presented in this work confirmed previous predictions; compound **14** is the most active of all compounds presented in this paper.

2.3. Analysis of the 3D structure–activity relationship

Detailed chemometric analysis was performed in order to elucidate the structural variables important for the anticancer activity of the analyzed compounds and, possibly, to gain deeper understanding of the molecular mechanism through which anticancer activity is achieved.

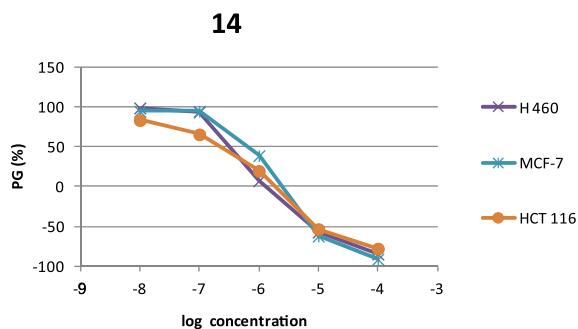


Fig. 2. The concentration–response curve of the most active compound **14**. PG = percentage of growth.

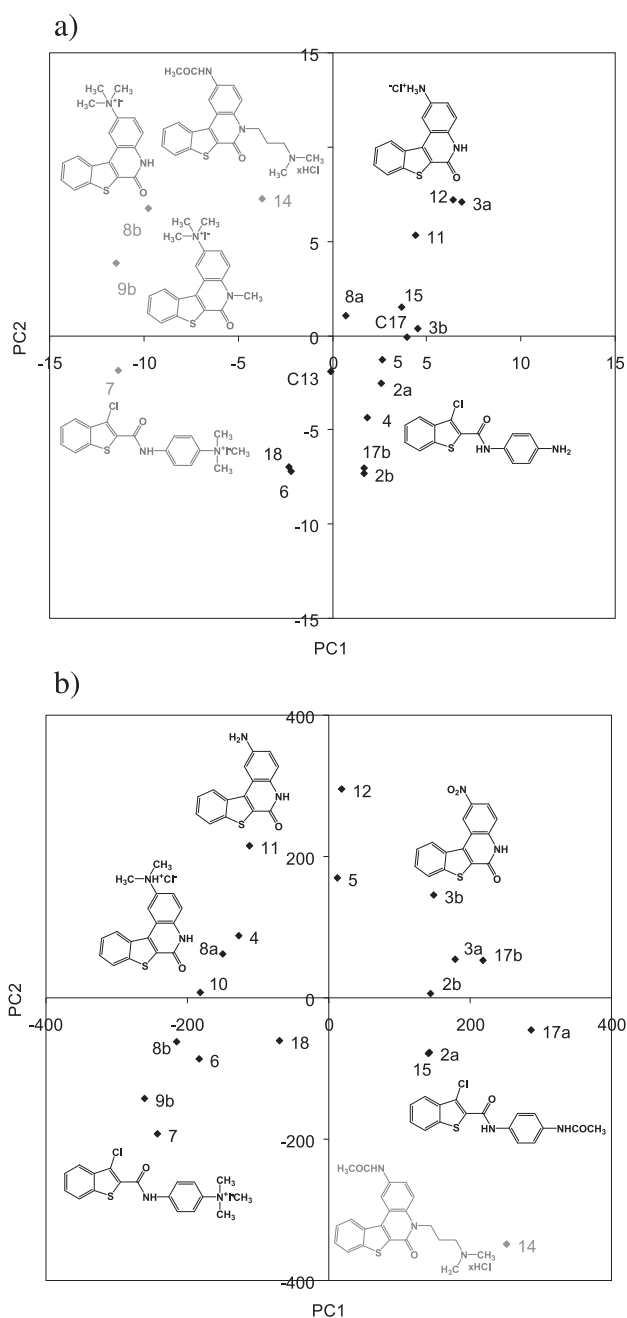


Fig. 3. PCA scoring plot using: a) autoscaling data, b) raw data.

2.3.1. Principal component analysis and 3D-derived QSAR models

Principal component analysis (PCA) was performed on the overall dataset of 19 compounds. The first two principal components explained 38% of variance in the case of autoscaled data and 72% in the case when the raw data was used. Distribution of the compounds in the PC space (PC scores) was examined in order to check similarity between the molecules and their possible grouping (Fig. 3). PCA is also useful tool for analyzing variation between the descriptors of the dataset. Since PCs are constructed in a way that the first few components describe majority of the variance among descriptors (X-matrix), their loadings describe descriptors with the highest contribution to the overall variance in the X-space (Supplemental material Fig. S3).

Using antitumor activity against HCT 116 (colon carcinoma) cells, 3D-derived QSAR models **1A** and **1B** were derived (Fig. S1a in

Supplement material and Fig. 4a, respectively). In case of model **1A**, autoscaling procedure was applied, while model **1B** was derived using raw data. 3D-derived QSAR models **2A** and **2B** were built using antitumor activity against MCF-7 (breast carcinoma) cells (Fig. S1b in Supplement material and Fig. 4b, respectively). Model **2A** was built using autoscaling procedure, while model **2B** was built using raw data. Statistical properties of derived models are summarized in Table 2.

Models **1A**, **1B**, **2A** and **2B** were derived using 17 compounds since compounds **8b** and **14** were identified as outliers and were

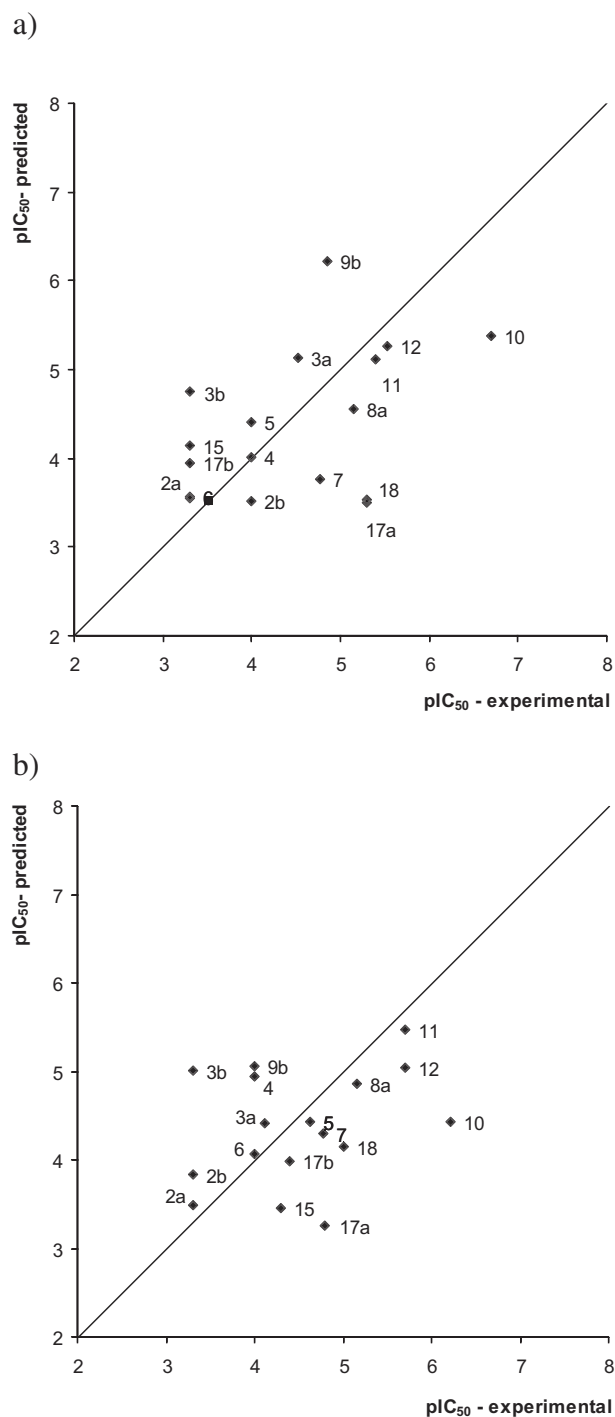


Fig. 4. Predicted vs. experimental antitumor activity (expressed as pIC₅₀) in case of: a) model **1B**, b) model **2B**.

omitted. Compound **8b** tends to precipitate and it is hard to determine its anticancer activity. In cases of HCT 116 and H460 cells it was only possible to estimate its IC₅₀ as larger than 100 μM, while in case of MCF cell line it was measured with an error of 92% (Table 1). Compound **14** was designed according to our previous QSAR analysis [25] and it was show to be the most active of all compounds presented in this paper. Differences in its chemical structure comparing to the rest of the presented compounds were recognized by statistical analysis. Principal component analysis (PCA) performed on raw data revealed its isolated position in the space of physico-chemical descriptors (Fig. 3b) and PLS analysis revealed it as an outlier in the derived models. Beside compounds **14** and **8b**, PCA performed on the autoscaled descriptors also clearly distinguished compounds **7** and **9b** from the rest of the compounds in the space of physico-chemical descriptors (Fig. 3a). In order to further improve quality of the models, compounds **7** and **9b** were also omitted from the training set. Predictive ability of such models was largely improved (values in brackets in Table 2 and Fig. S2 in Supplement material) comparing to the models built using 17 compounds.

2.3.2. Molecular descriptors with the highest impact on the antitumor activity

PCA loadings plot (Supplement material Fig. S3) revealed following descriptors as the ones with the highest variation among the studied compounds: W1–W3 (hydrophilic regions), V (volume), WN1 (H-bond acceptor descriptor, calculated with amide group as the probe), S (surface), HSA (the sum of hydrophobic surface areas), WO1 (H-bond donor descriptor, calculated with carbonyl oxygen as the probe) and %FU4–%FU8 (the percentage of unionized species calculated at pH 4, 5, 6, 7 and 8).

Partial Least Square (PLS) analysis provides information on quantitative influence of each descriptor to the derived QSAR models. In case of models derived using autoscaling procedure, influence of each descriptor to the compound's activity can be estimated directly from its PLS coefficient. In case of models derived using raw data matrix, the real impact of a descriptor on the biological activity is given as the product of the descriptor's value and its PLS coefficient. From autoscaling models **1A** and **2A** (Fig. 5) descriptors related to the solubility properties (LgS10, L4LgS) and hydrophobic regions (CD8–CD6, D8, D7) were identified as the descriptors that have the highest positive influence on compound's anticancer activity. The same observation was experimentally confirmed since the major obstacle for testing anticancer activity of presented compounds was their low solubility. The same models identified descriptors related to the molecular flexibility (FLEX, FLEX RB, G) as descriptors that decrease anticancer activity of investigated compounds. The later implies that decrease in compound's flexibility should increase its anticancer activity.

Models obtained using raw data, **1B** and **2B** identified solubility (LOlgS) and metabolic stability (MetStab) as descriptors that increase anticancer activity of investigated compounds (Fig. 6). Polarizability and dispersion forces (W1–W3), sum of hydrophobic surfaces (HSA), molecular mass (MW) and surface (S) were determined as descriptors with negative impact on anticancer activity by models **1B** and **2B**. Interestingly, while possibility of compounds to accept H-bond (WN1) and percentage of unionized species at pH 7 (%FU7) are according to model **1B** descriptors that improve anticancer activity of the studied compounds, model **2B** identified them as descriptors that are negatively correlated with antitumor activity. This might indicate that optimal antitumor activities toward HCT 116 and MCF-7 cell lines are achieved through different molecular mechanisms.

In our previous studies, accomplished for different datasets of amides and quinolones [18,25], V (volume), S (surface) and HSA

Table 1
IC₅₀ values (in μM) of compounds **2a–18**.

Compounds	IC ₅₀ ^a (μM)		
	Cell lines		
Scheme 1	HCT116	MCF-7	H460
2a	>100	>100	>100
2b	≥100 ^b	>100 ^b	55 ± 38 ^b
3a	30 ± 9	76 ± 23	>100
3b	22 ± 4	49 ± 31	18 ± 2
4	≥100	≥100	>100
5	≥100	24 ± 24	>100
6	>100 ^b	>100 ^b	>100 ^b
7	17 ± 2	17 ± 2	20 ± 7
8a	7 ± 1	7 ± 1	37 ± 35
8b	>100	50 ± 46	>100
9b	5 ± 0.4	10 ± 3	18 ± 3
10	5 ± 1	16 ± 1	13 ± 1
11	4 ± 0.2	2 ± 1	9 ± 3
12	3 ± 0.2	2 ± 0.1	6 ± 2
14	0.2 ± 0.002	0.6 ± 0.3	0.3 ± 0.06
15	14 ± 0.7	≥100	40 ± 24
17a	≥100	>100	>100
17b	>100 ^b	≥100 ^b	>100 ^b
18	>100	>100	>100

^a IC₅₀: the concentration that causes 50% growth inhibition.

^b The precipitates interfered with the MTT test.

(sum of hydrophobic surfaces) were identified as descriptors that are positively correlated with antitumor activity at MCF-7 cell line, while according to this study (models **1B** and **2B**) they have negative impact on antitumor activity. Average values of these descriptors for the dataset compounds are significantly lower in case of the compounds presented in this paper ($V = 657.5 \text{ \AA}^3$, $S = 446.7 \text{ \AA}^2$, $HSA = 381.8 \text{ \AA}^2$) comparing to the average values of the compounds used in previous studies ($V = 759.3 \text{ \AA}^3$, $S = 517.9 \text{ \AA}^2$, $HSA = 438.0 \text{ \AA}^2$). Apparently, increase of the size of the presented compounds should increase their anticancer activities toward MCF-7 cell line. Descriptors with the highest negative impact on antitumor activity for the presented compounds (the same cell line, MCF-7) are common with the descriptors found for the previous two groups of compounds: W1–W2 (hydrophilic volumes describing polarizability and dispersion forces), WO1 (H-bond donor descriptor, calculated with carbonyl group as the probe), WN1 (H-bond acceptor descriptor, calculated with amide group as the probe). Further decrease of these descriptors should lead to further increase of the compound's anticancer activity against MCF-7 cells. According to models derived using autoscaling procedure, descriptors related to the solubility (L2LgS, L3LgS, L4LgS) positively

Table 2
Statistical properties of 3D-derived QSAR models.

Model	nO ^a	nLV ^b	R ²	SDEC ^c	Q ^{2d}	SDEP ^e
1A	17 (15) ^f	1 (5) ^f	0.77 (0.98) ^f	0.37 (0.10) ^f	0.58 (0.87) ^f	0.51 (0.29) ^f
1B	17 (15) ^f	7 (6) ^f	0.95 (0.98) ^f	0.17 (0.12) ^f	0.62 (0.84) ^f	0.48 (0.32) ^f
2A	17 (15) ^f	8 (6) ^f	0.99 (0.99) ^f	0.07 (0.07) ^f	0.69 (0.73) ^f	0.41 (0.39) ^f
2B	17 (15) ^f	3 (2) ^f	0.79 (0.76) ^f	0.33 (0.37) ^f	0.58 (0.58) ^f	0.47 (0.49) ^f

^a Number of objects used to build the model.

^b Number of latent variables.

^c SDEC is standard deviation of error of calculation.

^d Q² is the cross-validated predictive performance and is given by $Q^2 = 1 - (\sum_{i=1}^n (y_{\text{exp}(i)} - y_{\text{pred}(i)})^2 / \sum_{i=1}^n (y_{\text{exp}(i)} - \langle y_{\text{exp}} \rangle)^2)$; where $y_{\text{pred}(i)}$ corresponds to the predicted and $y_{\text{exp}(i)}$ to the experimentally determined inhibition, pIC₅₀ for the compound i , respectively.

^e SDEP is the standard deviation in cross-validated prediction and is given by $SDEP = \sqrt{(\sum_{i=1}^n (y_{\text{exp}(i)} - y_{\text{pred}(i)})^2 / n)}$.

^f Calculations for the model in which two additional outliers (**7**, **9b**) have been expelled.

affect antitumor activity for of all compounds: those presented here as well as amidino-substituted amides and quinolones studied earlier. These finding was also experimentally observed since low solubility of investigated compounds often presents the largest obstacle in obtaining active compounds. Thus, increase in compound's solubility should increase its anticancer activity.

3. Molecular mechanism of action

As part of their molecular mechanism of action, some compounds were evaluated for their DNA binding properties. In a general manner, binding to DNA correlates with a stabilization of the hybridization of the two strands of the helix that could be visualized as part of the increase of the temperature that is required to separate the two strands. DNA melting temperature studies are commonly performed with this purpose as a quick and informative tool for DNA binding. Calf thymus DNA (CT-DNA) was incubated alone or with a fixed concentration of each compound and the absorbance was measured using a reference cuvette containing the same buffer alone or with the same compound at the same concentration to only get an insight on the hyperchromicity associated with DNA, but not with the compound itself. From this series, only the quinolones **8b** and **14** present a strong DNA binding propensity, as evidenced by increase of the temperature of 10 °C (ΔT_m) for a drug/DNA ratio R of only 0.25, and up to 16.9 °C and 19 °C, respectively, at $R = 1$ (Table 3). By contrast, the quinolone iodide **9b** presents much weaker ΔT_m value. Similarly, the quinolones **10** and **11** as well as the carboxianilide **7** only have low DNA binding properties. Therefore, among the carboxianilides, only compound **7** presents some DNA binding propensity. Interestingly, this compound was also the most active carboxianilide on cells as evidenced in MTT assays (Table 1). Finally, compounds **2a–b**, **3a**, **4–6**, **8a** and **12** failed to protect the DNA helix from heat-induced destabilization suggesting no DNA binding propensity (data not shown). In terms of structure activity relationships, the addition of a methyl group on the quinolone iodine **8b** to give **9b** decreases the efficacy of DNA binding with the ΔT_m value that drops from 16.9 to 5.9 °C and the fully relaxed plasmid DNA that appeared at 0.5 μM using **8b**, but 20 μM using **9b**. However, this conclusion does not apply to the protonated *N,N*-dimethylamino substituted quinolone **8a** which does not intercalate nor bind DNA whereas the protonated *N,N*-dimethylamino substituted *N*-methyl-quinolone **10** present some (even if weak) DNA binding properties and weakly intercalates.

UV/visible spectra analyses of the absorbancy was measured using the various tested compounds (20 μM) in the absence or presence of increasing concentrations from 1 to 100 μM of CT-DNA (top to bottom).

Comparison of the spectra in the absence (dashed lanes) and presence of 100 μM of CT-DNA (dotted lanes) evidenced strong hypochromic effect ranging from 23% to 58% upon binding to the DNA (Fig. 7). The hypochromic effect is associated with a bathochromic effect (red shifts) using the most efficient DNA binding compounds **8b**, **9b** and **14** as exemplified by the increase of maximum wavelength ($\Delta\lambda$) of up to 6 nm at the upper CT-DNA concentration (drug/DNA ration of 0.2).

Induced red shift associated with hypochromic effect suggests interaction of the aromatic system of compounds **8b**, **9b** and **14** with the base pairs. Therefore the compounds were evaluated for DNA intercalation properties using the properties of topoisomerase I to differentially relax supercoiled DNA in the presence of DNA intercalators [26]. All compounds were evaluated at the same concentration range from 1 to 50 μM (Fig. 8) and the concentration was then adjusted for the strongest DNA intercalating compounds to lower concentrations from 0.2 to 5 μM (Fig. 8, bottom panel).

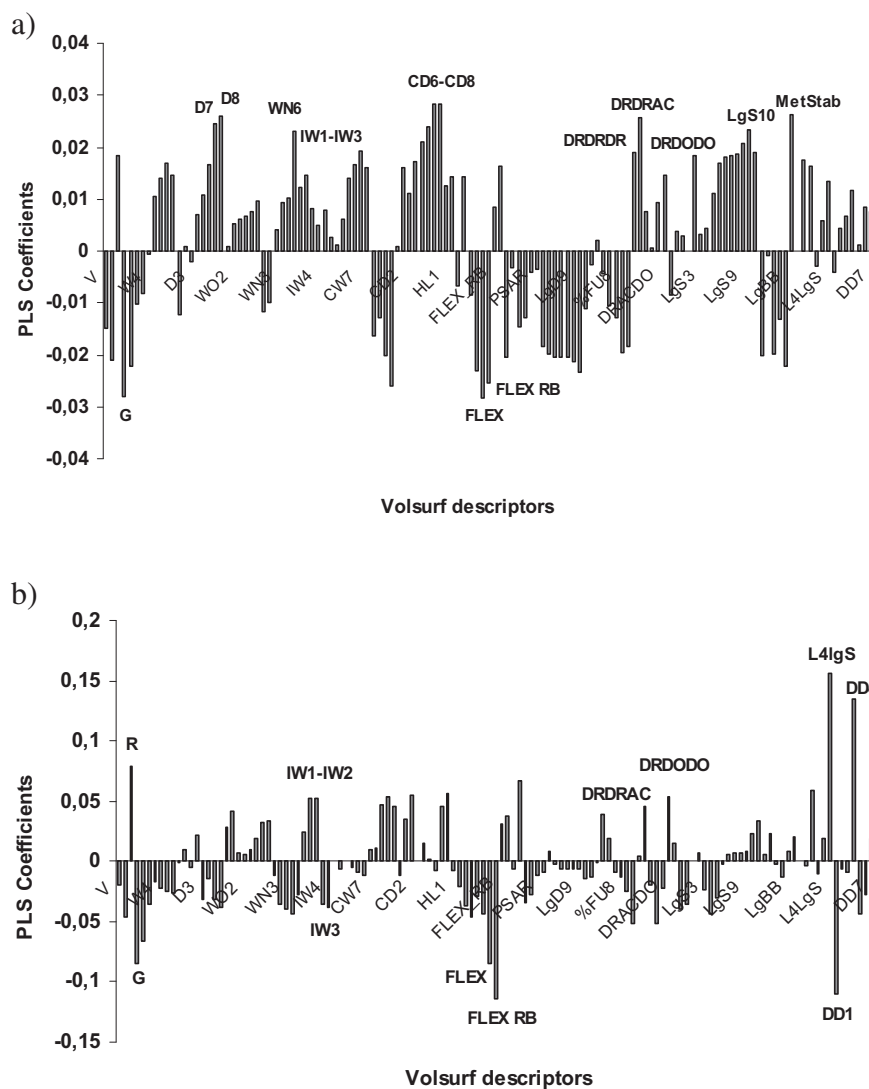


Fig. 5. PLS coefficients of 3D-derived QSAR model: a) **1A**, b) **2A**. Descriptors with the highest impact on the activity are labeled; list and description of all 128 Volsurf + descriptors is given in the Volsurf + manual [27].

From this experiment, three type of compounds could be classified depending on their DNA base pair intercalation efficiency. As a first group, the carboxianilide **4**, as well as the quinolones **3b** and **8a** do not intercalate at all into the DNA helix. In a second group, the quinolones **3a**, **10–12** as well as the carboxianilide **7** evidence weak DNA intercalating properties as visualized by fully relaxed plasmid DNAs obtained using 20–50 μM of compounds. The last group contains the quinolones **9b**, **8b** and **14** as efficient DNA intercalators. This is in agreement with both the increase of the DNA melting temperature (Table 3) and the red shifts of the peaks of absorbance obtained in UV/Visible spectroscopy measurements (Fig. 7). Particularly, compounds **8b** and **14** are highly efficient DNA intercalators with fully relaxed circular DNA (*Rel* form, Fig. 8 bottom panel) generated in the presence of only 0.5–1 μM of drug. Those two compounds presented the highest DNA stabilization properties with more than 10 $^{\circ}\text{C}$ required for DNA denaturation from the weaker evaluated drug/DNA ratio ($R = 0.25$) to the highest one ($R = 1$) (Table 3).

Compounds **9b**, **8b** and **14** were therefore evaluated for potential modifications of the circular dichroism (CD) spectra for CT-DNA, but none of those compounds clearly evidenced typical negative induced CD (ICD) attempted for a DNA intercalating compound

(data not shown). Compounds **7**, **10**, **11** and **14** induce a change in the intensity of the positive (275 nm) and/or the negative (245 nm) peaks of the CD spectra for normal B-DNA conformation, suggesting modifications in the base stacking and the ellipticity of the DNA helix.

Based on the absence of isosbestic points in UV/Visible titration studies using those compounds (Fig. 7), it was attempted that compounds **9b**, **8b** and **14** do not present a single binding mode. The DNA relaxation assay is a functional test. It clearly evidenced those drugs as potent and functional DNA intercalators. By contrast, circular dichroism experiment, as a biophysical analysis, gives structural information on the orientation of the compound relatively to the DNA helix (groove binding, intercalation between adjacent base pairs). Thus, the absence of ICD suggests that the intercalation evidenced using the topoisomerase I-induced DNA relaxation experiment may be associated with another mode of binding such as interaction with the phosphate backbone using the positively charges arms (quaternary ammonium substituent for **8b** and **9b** or protonated *N,N*-dimethylamino-propyl for **14**), interfering with correct intercalation of the planar chromophore between adjacent base pairs that therefore could not result in a negative ICD.

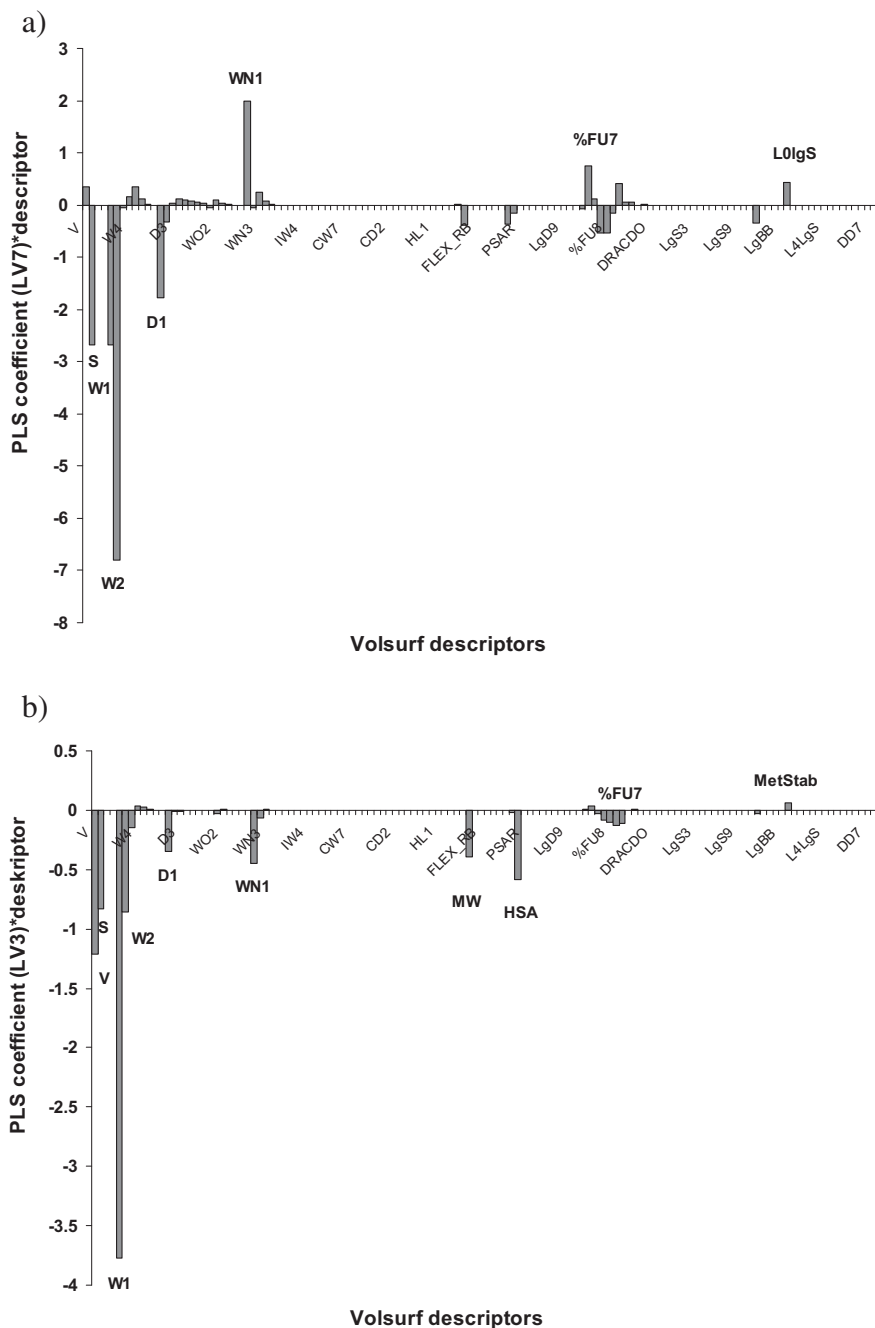


Fig. 6. Products of the descriptors average value (calculated for the dataset used to build the model) and the associated PLS coefficient of 3D-derived QSAR model: a) **1B** and b) **2B**. Descriptors with the highest impact on the activity are labeled; list and description of all 128 Volsurf + descriptors is given in the Volsurf + manual [27].

In order to further evaluate the mode of binding to DNA of this new series of compounds, we then used DNaseI footprinting assays to assess if their potential sequence selectivity. Compounds **8b** and **14** did not reveal any sequence-selective binding but non-selective binding inducing a global inhibition of DNaseI cleavage along the whole DNA sequence using 2–5 μM of compound (Supplement material Fig. S4). Compound **9b** gave similar global inhibition, starting at much higher concentration (data not shown) in agreement with a weaker DNA binding propensity as evidenced using thermal melting temperature studies (Table 3).

Since DNA intercalation could result in an inhibition of topoisomerases DNA cleavage activities, we finally looked at topoisomerases inhibition. For topoisomerase I, topoisomerase I-

Table 3
DNA melting temperature for CT-DNA incubated with the indicated compounds at the various drug/DNA ratio (*R*).

Drug/DNA ratio	ΔT_m ($^{\circ}\text{C}$)					
	7	8b	9b	10	11	14
<i>R</i> = 0.25		10				10
<i>R</i> = 0.5	1	12.8	2.9	0	2	12.7
<i>R</i> = 1	3	16.9	5.9	3	^a P	19

^a P = precipitation.

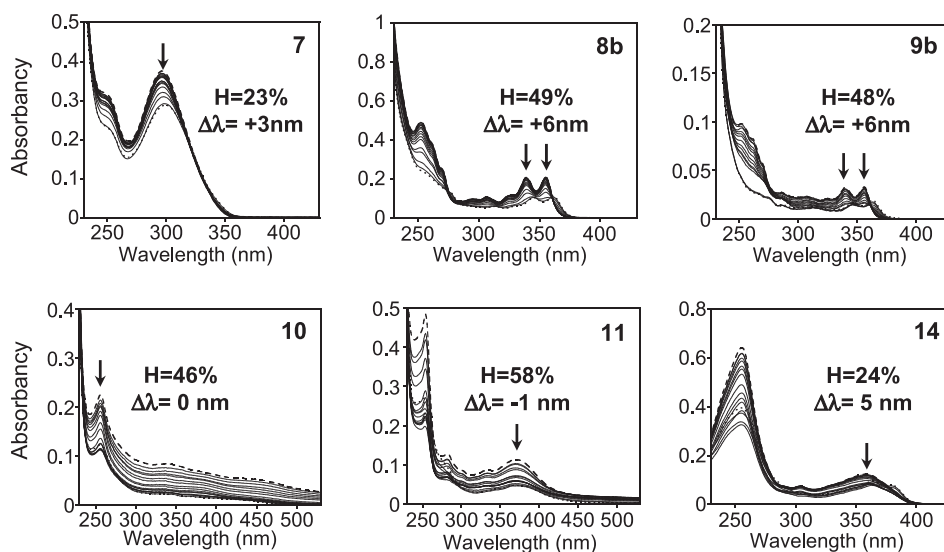


Fig. 7. UV/Visible spectra analyses of the binding to DNA of selected compounds. Compounds selected from thermal melting temperature studies (20 μM) were incubated in BPE buffer with or without increasing concentrations of CT-DNA from 0.1 to 100 μM . Spectra were collected against a cuvette containing the same concentration of CT-DNA in the same buffer to subtract the absorbance of CT-DNA in the course of the acquisition process. Dashed lanes correspond to samples containing the drug without CT-DNA; plain lanes to the addition of CT-DNA (0, 0.1, 0.2, 0.4, 0.6, 0.8, 1, 2, 4, 6, 8, 10, 20, 40, 60, 80 μM , top to bottom); dotted lanes to the addition of 100 μM of CT-DNA; H is the percentage of hypochromicity; $\Delta\lambda$ is the wavelength shift at the indicated arrows where $\Delta\lambda = \lambda_{\text{peak}}(100\mu\text{M CT-DNA}) - \lambda_{\text{peak}}(\text{drug alone})$.

induced DNA relaxation assays failed to evidence any accumulation of nicked DNA that should co-migrate with the nicked form (Fig. 8). None of the compounds evidenced an accumulation of the upper band which intensity is similar to that obtained in the lanes containing the DNA alone (“DNA”) or incubated with topoisomerase I in the absence of any compounds (lanes “0” and “Topo I”), even at the highest drug concentrations, suggesting that none of those compounds are potent topoisomerase I poisoning drugs.

We then focussed on topoisomerase II as a target. Inhibition of topoisomerase II is revealed by the generation of a linear band when the compound is a poison of topoisomerase II, as obtained using the reference drug etoposide used as a positive control (Fig. 9). This latter effect is not visualized using those compounds suggesting that none of them are topoisomerase II inhibitors. Only compound 7 presents a small increase in the linear band using 50 μM of compound.

The DNA binding studies clearly evidence the quinolones 8b and 14 as strong DNA intercalators, the *N*-methyl-quinolone 9b as a medium intercalator whereas the quinolones 10, 11 and 12 as well the carboxanilide 7 are much weaker DNA intercalators.

PCA analysis (Fig. 3) clearly distinguished compounds 14, 8b and 9b from the rest of the investigated compounds in the space of molecular descriptors. In order to identify molecular properties responsible for the differences in DNA binding properties of investigated compounds, we compared their descriptors with the descriptors found for the rest of investigated compounds (Table 4, Fig. S5 in the supplement). The largest differences are between the descriptors related to percentage of unionized species at pH 4–8 (%FU4–8). The lower values of %FU4–8 descriptors enhance compound’s DNA binding properties, which is understandable since compound’s preference to exist in ionized (positively charged) form should enhance its interaction with DNA.

Previous 3D-QSAR analysis [18] pointed to the integrity moments, which indicate concentration of hydrophilic regions on one part of the molecule, and 3D pharmacophoric descriptors related to the hydrogen bond formation potency as the descriptors that are positively correlated with the biological activity. These descriptors, combined with the large planar platform, are desirable for DNA

binders. In the QSAR analysis presented in this paper, these descriptors were also found to be positively correlated with compound’s activity (Fig. 5) by models 1A and 2A. Further, integrity moments of compounds 8b (IW1 = 0.09, IW2 = 0.42, IW3 = 1.21) and 14 (IW1 = 0.12, IW2 = 0.48, IW3 = 1.27), which are the only compounds from this series that present a strong DNA binding propensity, are significantly higher than the average integrity moments of the rest of the compounds presented in this paper (IW1 = 0.07, IW2 = 0.21, IW3 = 0.71). The same is partly true for 3D pharmacophoric descriptors related to H-bonding: DRDRDO (8b: 0.00, 14: 21.7, average: 14.9), DRDRDR (8b: 27.4, 14: 22.2, average: 18.2), DRACDO (8b: 0.00, 14: 12.2, average: 16.4), DRDODO (8b: 0.00, 14: 0.00, average: 7.34), DRDRAC (8b: 26.7, 14: 26.9, average: 20.2). Thus, previous and presented chemometric analyses are in agreement and are supported by experimental results since compounds that were experimentally found as DNA binders are discriminated from the rest of the compounds by the same descriptors in both analyses [18].

4. Conclusions

Novel compounds from the benzothiophene and thienothiophene series with nitrogen-bearing substituents were synthesized and tested on three tumor cell lines. The majority of the compounds was slightly soluble and exerted low to modest antiproliferative effect. All carboxanilides, except 7 were less active compared to the quinolones prepared from them. The most active quinolones were 8a, 9b, 10–12 and 14. Compound 14 was the most active compound from this series, having the IC_{50} concentrations $\approx 0.3 \mu\text{M}$. Since this compound was designed by previous QSAR analysis and predicted as active compound it presents an excellent example of verification of chemometric analysis by laboratory methods.

Detailed chemometric analysis was performed on the dataset consisting of the investigated compounds. The 3D-derived QSAR analysis and PCA enabled identification of the descriptors important for anticancer activity of investigated compounds. Solubility, metabolic stability and the possibility of the compound to be ionized at pH 4–8 were found as molecular properties whose increase should lead

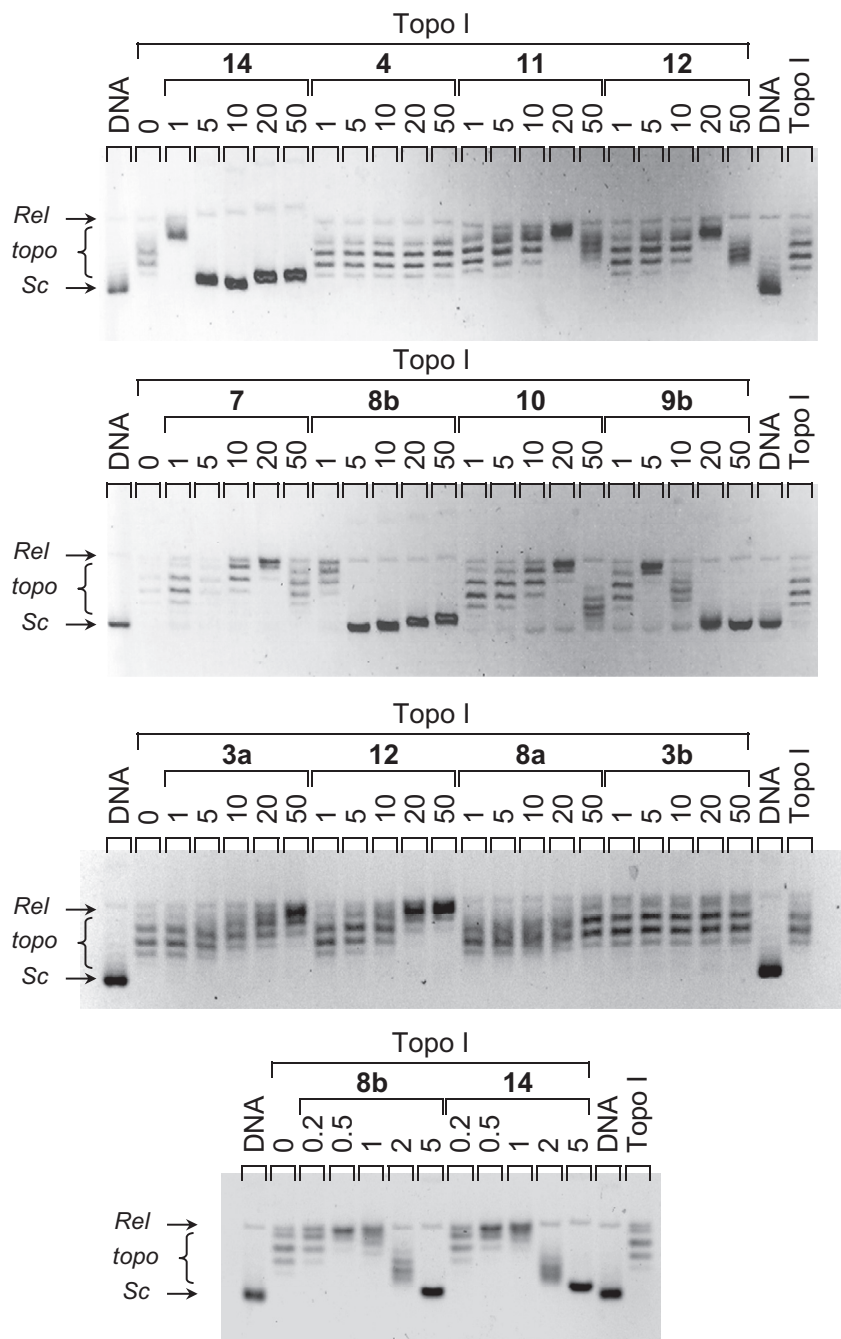


Fig. 8. Topoisomerase I-induced DNA relaxation. Supercoiled pUC19 plasmid was incubated or not ("0" lanes) with increasing concentrations of the indicated compounds at the concentration specified on the top of each lanes (μM) prior to be subjected to relaxation using topoisomerase I ("Topo I"). DNA samples were separated on an agarose gel that was post-stained using ethidium bromide to visualize the different circular DNA bands (Sc, supercoiled; topo, topoisomers; Rel, relaxed DNA). "DNA", supercoiled plasmid untreated with topoisomerase I).

to increase of anticancer activity of the investigated compounds. Molecular flexibility, polarizability and sum of hydrophobic surfaces were recognized as the descriptors whose decrease should lead to increase of anticancer activity of the investigated compounds. This findings can be used as guidelines in designing new compounds with increased anticancer activity, similarly as previous QSAR analysis was used for designing of compound **14**.

The DNA binding propensities of studied compounds (anilides **2a–b**, **4–7** and quinolones **3a–b**, **8a**, **10–14**) were investigated using DNA melting temperature studies, UV/Visible spectrophotometry, CD spectrometry and inhibition of topoisomerase I and II

tests. Compounds **8b**, **9b** and **14** were identified as the compounds with strong DNA binding propensity. The same compounds were distinguished from the rest of the compounds by chemometric tools (PCA and PLS analysis). The highest difference in their molecular properties comparing to the rest of the compounds were found in their possibility to exist in ionized form at pH 4–8, concentration of hydrophilic regions on one part of the molecule and their hydrogen bond formation potency. These descriptors, combined with the large planar platform, are desirable for DNA binders and should be considered in future attempts to design DNA binders.

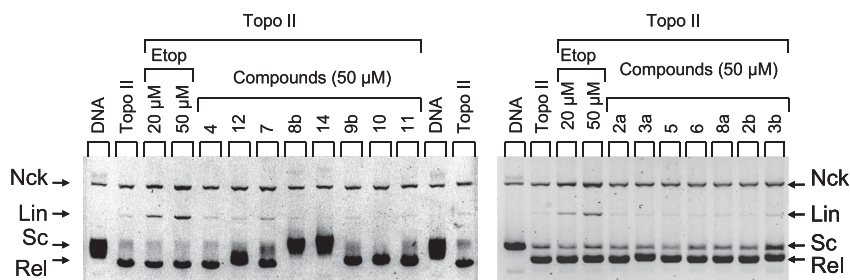


Fig. 9. Topoisomerase II-induced poisoning effect. Supercoiled pUC19 plasmid was incubated or not ("DNA" lanes) with the indicated compounds at the concentration specified on the top of each lanes prior to be subjected to DNA cleavage by topoisomerase II ("Topo II"). Etoposide ("Etop" lanes) was used as a positive control for topoisomerase II poisoning. DNA samples were separated on an agarose gel containing ethidium bromide to visualize the different DNA forms (Nck, nicked DNA; Lin, linear DNA; Sc, supercoiled plasmid; Rel, relaxed DNA).

5. Experimental

5.1. Chemistry

Melting points were recorded SMP11 Bibby and Büchi 535 apparatus and are uncorrected. IR spectra were recorded on FTIR-ATR spectrophotometer. ^1H and ^{13}C NMR spectra were recorded on Varian Gemini 300 or Varian Gemini 600 spectrophotometers at 300, 600, 150 and 75 MHz, respectively. All NMR spectra were measured in $\text{DMSO-}d_6$ solutions using TMS as an internal standard. Elemental analyses for carbon, hydrogen and nitrogen were performed on a Perkin–Elmer 2400 elemental analyzer and a Perkin–Elmer, Series II, CHNS analyzer 2400. All compounds were routinely checked by TLC with Merck silica gel 60F-254 glass plates. In preparative photochemical experiments the irradiation was performed at room temperature with a water-cooled immersion well with an "Origin Hanau" 400 W high pressure mercury arc lamp using Pyrex glass as a cut-off filter of wavelengths below 280 nm.

5.1.1. General method for the synthesis of substituted 6-oxo-5,6-dihydro [1]benzothieno[2,3-*c*]quinolines (**3a–b**) and 6-oxo-5,6-dihydrothieno[3',2':4,5]thienyl[2,3-*c*]quinoline (**19**)

A solution of *N*-substituted 3-chlorobenzo[*b*]thiophene-2-carboxamide derivatives (**2a–b**) in methanol/toluene was irradiated at room temperature with a 400-W high pressure mercury lamp for 2.5–10 h. The solution was concentrated and the obtained solid was filtered off.

5.1.1.1. 2-Acetamido-6-oxo-5,6-dihydro [1]benzothieno[2,3-*c*]quinoline 3a. A solution of **2a** (0.10 g, 0.29 mmol) in methanol (15 ml) and toluene (20 ml) was irradiated for 2.5 h, 0.05 g (56%) of white solid was obtained; m.p. $>300^\circ\text{C}$; IR ν/cm^{-1} : 3263, 3111, 1651, 1605, 1566; ^1H NMR (300 MHz, $\text{DMSO-}d_6$) (δ ppm): 12.21 (s, 1H, $\text{H}_{\text{quinolone}}$), 10.23 (s, 1H, H_{amide}), 9.17 (d, 1H, $J = 1.7$ Hz, $\text{H}_{\text{arom.}}$), 8.76 (d, 1H, $J = 7.4$ Hz, $\text{H}_{\text{arom.}}$), 8.29 (dd, 1H, $J_1 = 7.1$ Hz, $J_2 = 1.7$ Hz, $\text{H}_{\text{arom.}}$), 7.79–7.67 (m, 3H, $\text{H}_{\text{arom.}}$), 7.49 (d, 1H, $J = 8.8$ Hz, $\text{H}_{\text{arom.}}$), 2.14 (s, 3H, CH_3); ^{13}C NMR (75 MHz, $\text{DMSO-}d_6$) (δ ppm): 169.0, 158.0, 141.9, 136.0, 135.8, 135.0, 133.8, 133.1, 127.9, 126.3, 125.3, 124.8, 120.8, 117.7, 117.3, 112.9, 24.6; elemental analysis calcd. (%) for $\text{C}_{17}\text{H}_{12}\text{N}_2\text{O}_2\text{S}$: C 66.22, H 3.92, N 9.08; found C 66.07, H 4.17, N 8.98.

5.1.1.2. 2-Nitro-6-oxo-5,6-dihydro [1]benzothieno[2,3-*c*]quinoline 3b. A solution of **2b** (0.10 g, 0.30 mmol) in methanol (15 ml) and toluene (25 ml) was irradiated for 3 h, 0.02 g (24%) of brown solid was obtained; m.p. $>300^\circ\text{C}$; IR ν/cm^{-1} : 2969, 2829, 1643, 1587, 1532; ^1H NMR (600 MHz, $\text{DMSO-}d_6$) (δ ppm): 12.78 (s, 1H, $\text{H}_{\text{quinolone}}$), 9.44 (s, 1H, $\text{H}_{\text{arom.}}$), 8.77 (d, 1H, $J = 7.6$ Hz, $\text{H}_{\text{arom.}}$), 8.43 (dd, 1H, $J_1 = 9.1$ Hz, $J_2 = 2.3$ Hz, $\text{H}_{\text{arom.}}$), 8.32 (d, 1H, $J = 8.0$ Hz, $\text{H}_{\text{arom.}}$), 7.80 (t, 1H, $J = 7.7$ Hz, $\text{H}_{\text{arom.}}$), 7.73 (t, 1H, $J = 7.6$ Hz, $\text{H}_{\text{arom.}}$), 7.70 (d, 1H,

$J = 9.1$ Hz, $\text{H}_{\text{arom.}}$); ^{13}C NMR (150 MHz, $\text{DMSO-}d_6$) (δ ppm): 158.0, 142.2, 142.0, 141.4, 134.8, 134, 7, 133.9, 127.9, 126.5, 125.0, 124.4, 123.6, 119.2, 117.5, 116.6; elemental analysis calcd. (%) for $\text{C}_{15}\text{H}_8\text{N}_2\text{O}_3\text{S}$: C 60.80, H 2.72, N 9.45; found C 61.08, H 2.52, N 9.60.

5.1.1.3. 2-Acetamido-6-oxo-5,6-dihydrothieno[3',2':4,5]thienyl[2,3-*c*]quinolin 19. A solution of **17a** (0.10 g, 0.29 mmol) in methanol (60 ml) and toluene (60 ml) was irradiated for 10 h. The solution was concentrated and the crude product was purified by column chromatography with dichloromethane–methanol mixture to obtain 0.03 g (28%) of ivory solid; m.p. $>300^\circ\text{C}$; IR ν/cm^{-1} : 3358, 3112, 1647, 1593; ^1H NMR (300 MHz, $\text{DMSO-}d_6$) (δ ppm): 12.00 (s, 1H, $\text{H}_{\text{quinolone}}$), 10.17 (s, 1H, H_{amide}), 8.86 (d, 1H, $J = 2.1$ Hz, $\text{H}_{\text{arom.}}$), 8.04 (d, 1H, $J = 5.3$ Hz, $\text{H}_{\text{thiophene}}$), 7.96 (d, 1H, $J = 5.4$ Hz, $\text{H}_{\text{thiophene}}$), 7.75 (dd, 1H, $J_1 = 8.9$ Hz, $J_2 = 2.1$ Hz, $\text{H}_{\text{arom.}}$), 7.45 (d, 1H, $J = 8.9$ Hz, $\text{H}_{\text{arom.}}$), 1.25 (s, 3H, CH_3); ^{13}C NMR (75 MHz, $\text{DMSO-}d_6$) (δ ppm): 165.4 (s), 159.3 (s), 143.9 (s), 138.6 (s), 136.2 (s), 133.9 (s), 132.7 (s), 131.5 (d), 130.7 (d), 128.3 (d), 121.2 (d), 119.0 (s), 117.6 (d), 116.3 (s), 24.5 (q); elemental analysis calcd. (%) for $\text{C}_{15}\text{H}_{10}\text{N}_2\text{O}_2\text{S}_2$: C 57.31, H 3.21, N 8.91; found C 57.43, H 3.11, N 9.15.

5.1.2. Preparation of *N*-(4'-aminophenyl)-3-chlorobenzo[*b*]thiophene-2-carboxamide **4**

A solution of **2b** (1.11 g, 3.33 mmol) in THF (70 ml) and 10% Pd–C (0.56 g) was hydrogenated until the required quantity of H_2 was taken up. The solution was filtered through Celite to remove catalyst and the solvent was removed under reduced pressure. The crude product was purified by recrystallization from ethanol to obtain 0.79 g (78%) of light yellow solid; m.p. 163–164 $^\circ\text{C}$; IR ν/cm^{-1} : 3309, 3190, 1628, 1596, 1533; ^1H NMR (300 MHz, $\text{DMSO-}d_6$) (δ ppm): 10.10 (s, 1H, H_{amide}), 8.15–8.12 (m, 1H, $\text{H}_{\text{arom.}}$), 7.94–7.91 (m, 1H, $\text{H}_{\text{arom.}}$), 7.62–7.59 (m, 2H, $\text{H}_{\text{arom.}}$), 7.36 (d, 2H, $J = 8.7$ Hz, $\text{H}_{\text{arom.}}$), 6.57 (d, 2H, $J = 8.7$ Hz, $\text{H}_{\text{arom.}}$), 5.05 (s, 2H, NH_2); ^{13}C NMR (75 MHz, $\text{DMSO-}d_6$) (δ ppm): 158.0, 145.8, 136.5, 135.8, 132.9, 127.3, 127.2, 126.0, 123.4, 122.4, 121.9, 118.7, 113.7 (3C); elemental analysis calcd. (%) for $\text{C}_{15}\text{H}_{11}\text{ClN}_2\text{OS}$: C 59.50, H 3.66, N 9.25; found C 59.62, H 3.53, N 9.45.

5.1.3. Preparation of *N*-[4'-(*N,N,N*-trimethylamino)phenyl]-3-chlorobenzo[*b*]thiophene-2-carboxamide iodide **7**

The suspension of **2c** (1.00 g, 3.02 mmol) in a mixture of acetone (120 ml) and diethyl ether (50 ml) was heated with methyl iodide (0.59 ml, 9.48 mmol) for 18 h. The solution was concentrated and the crude product was filtered off and washed with diethyl ether to obtain 0.98 g (69%) of white solid; m.p. 227–230 $^\circ\text{C}$; IR ν/cm^{-1} : 3396, 3003, 1651, 1610, 1537; ^1H NMR (300 MHz, $\text{DMSO-}d_6$) (δ ppm): 10.89 (s, 1H, H_{amide}), 8.21–8.18 (m, 1H, $\text{H}_{\text{arom.}}$), 8.02–7.91 (m, 5H, $\text{H}_{\text{arom.}}$), 7.68–7.64 (m, 2H, $\text{H}_{\text{arom.}}$), 3.62 (s, 9H, CH_3); ^{13}C NMR (75 MHz, $\text{DMSO-}d_6$) (δ ppm): 159.5, 142.8, 139.3, 136.8, 135.6, 131.4,

Table 4

The average values of the descriptors that differ the most between the DNA intercalators (compounds **14**, **8b** and **9b**) and the rest of the compounds.

Descriptor ^a	Average value for compounds 14 , 8b and 9b	Average value for the rest of compounds presented in this paper	Average value for the previously investigated compounds
V/Å ³	749.9	654.2	759.3
S/Å ²	498.2	445.5	517.9
W1/Å ³	1209.8	1158.7	1308.5
W2/Å ³	669.0	715.0	788.4
W3/Å ³	328.6	383.6	425.8
WO1/Å ³	100.7	139.0	197.0
MW	342.4	316.8	364.7
HSA/Å ²	445.2	379.0	438.0
%FU4/%	0.00017	72.2	19.6
%FU5/%	0.00170	80.9	19.8
%FU6/%	0.01699	88.9	20.4
%FU7/%	0.16911	92.8	20.6
%FU8/%	1.61728	91.3	20.0

^a V, volume; S, surface; W1–W3, hydrophilic volumes describing polarizability and dispersion forces; WO1, H-bond donor descriptor calculated with carbonyl oxygen as the probe; MW, molecular mass; HSA, sum of hydrophobic surfaces; %FU4–%FU8, percentage of unionized species at pH 4–8.

127.8, 126.2, 123.6, 122.6, 121.3 (2C), 120.7 (2C), 120.2, 56.5 (3C); elemental analysis calcd. (%) for C₁₈H₁₈ClN₂O₅: C 45.73, H 3.84, N 5.93; found C 46.01, H 3.60, N 6.07.

5.1.4. Preparation of 2-(*N,N*-dimethylamino)-6-oxo-5,6-dihydro [1]benzothieno[2,3-*c*]quinoline hydrochloride **8a**

A solution of **6** (0.91 g, 2.48 mmol) in methanol (160 ml) and toluene (160 ml) was irradiated for 3 h. The solution was concentrated and the crude product was purified by column chromatography with dichloromethane–methanol mixture to obtain 0.28 g (35%) of brown solid; m.p. >300 °C; IR ν /cm⁻¹: 3392, 3224, 1652; ¹H NMR (300 MHz, DMSO-*d*₆) (δ ppm): 12.35 (s, 1H, H_{quinolone}), 8.95 (m, 1H, H_{arom.}), 8.77 (s, 1H, H_{arom.}), 8.31–8.28 (m, 1H, H_{arom.}), 7.73–7.62 (m, 4H, H_{arom.}), 3.72 (bs, 1H, NH⁺), 3.22 (s, 6H, CH₃); ¹³C NMR (75 MHz, DMSO-*d*₆) (δ ppm): 158.0, 142.2, 141.8, 136.0, 135.8, 135.7, 133.7, 128.1, 126.5 (2C), 126.0, 124.7, 119.4, 118.5, 118.1, 44.4 (2C); elemental analysis calcd. (%) for C₁₇H₁₅ClN₂O₅: C 61.72, H 4.57, N 8.47; found C 62.06, H 4.26, N 8.70.

5.1.5. Preparation of 2-(*N,N,N*-trimethylamino)-6-oxo-5,6-dihydro [1]benzothieno[2,3-*c*]quinoline iodide **8b**

A solution of **7** (0.20 g, 0.42 mmol) in ethanol (80 ml) and water (80 ml) was irradiated for 2 h, 0.15 g (81%) of white solid was obtained; m.p. >300 °C; IR ν /cm⁻¹: 3473, 3125, 3006, 1643; ¹H NMR (300 MHz, DMSO-*d*₆) (δ ppm): 12.59 (s, 1H, H_{quinolone}), 8.97–8.94 (m, 1H, H_{arom.}), 8.89 (d, 1H, *J* = 2.5 Hz, H_{arom.}), 8.35–8.32 (m, 1H, H_{arom.}), 8.24 (dd, 1H, *J*₁ = 9.3 Hz, *J*₂ = 2.5 Hz, H_{arom.}), 7.79–7.76 (m, 2H, H_{arom.}), 7.73 (d, 1H, *J* = 9.3 Hz, H_{arom.}), 3.79 (s, 9H, CH₃); ¹³C NMR (75 MHz, DMSO-*d*₆) (δ ppm): 158.3, 141.9, 141.7, 138.3, 135.5, 135.1, 134.3, 128.3, 126.7, 126.5, 124.7, 121.6, 118.5, 117.4, 115.6, 57.3 (3C); elemental analysis calcd. (%) for C₁₈H₁₇IN₂O₅: C 49.55, H 3.93, N 6.42; found C 49.30, H 4.19, N 6.15.

5.1.6. General method for the synthesis of 5-methyl-6-oxo-5,6-dihydro [1]benzothieno[2,3-*c*]quinolines (**9a–b**, **15**)

To a cold solution of corresponding quinolin-6-ones in anhydrous DMF, sodium hydride as 60–65% oil dispersion was added in two portions. After stirring for 15 min, methyl iodide was added to the solution and the reaction mixture was stirred for 2 h at 0–5 °C and 24 h at room temperature. The products were filtered off and recrystallized from ethanol.

5.1.6.1. 2-(*N,N*-dimethylamino)-5-methyl-6-oxo-5,6-dihydro [1]benzothieno[2,3-*c*]quinoline **9a**. From **8a** (0.27 g, 0.62 mmol) in DMF (10 ml), sodium hydride (0.13 g, 5.34 mmol) and methyl iodide (0.09 g, 0.61 mmol), after recrystallization from ethanol 0.06 g (20%) of light brown solid was obtained; m.p. >300 °C; IR ν /cm⁻¹: 3029, 2885, 2516, 1618, 1564; ¹H NMR (300 MHz, DMSO-*d*₆) (δ ppm): 8.72 (d, 1H, *J* = 8.4 Hz, H_{arom.}), 8.24 (d, 1H, *J* = 8.3 Hz, H_{arom.}), 7.84 (s, 1H, H_{arom.}), 7.73–7.66 (m, 2H, H_{arom.}), 7.62 (d, 1H, *J* = 9.4 Hz, H_{arom.}), 7.25 (d, 1H, *J* = 9.2 Hz, H_{arom.}), 3.77 (s, 3H, CH₃), 3.09 (s, 6H, CH₃); ¹³C NMR (75 MHz, DMSO-*d*₆) (δ ppm): 158.2, 141.7, 141.3, 138.3, 135.8, 133.9, 132.8, 127.5, 126.1 (2C), 125.7, 124.2 (2C), 118.3, 117.7, 44.6 (2C), 30.3; elemental analysis calcd. (%) for C₁₈H₁₆N₂O₅: C 70.10, H 5.23, N 9.08; found C 69.96, H 5.47, N 9.32.

5.1.6.2. 5-Methyl-2-(*N,N,N*-trimethylamino)-6-oxo-5,6-dihydro [1]benzothieno[2,3-*c*]quinoline iodide **9b**. From **8b** (0.27 g, 0.62 mmol) in DMF (10 ml), sodium hydride (0.13 g, 5.34 mmol) and methyl iodide (0.09 g, 0.61 mmol), after recrystallization from ethanol 0.06 g (20%) of white solid was obtained; m.p. 278–282 °C; IR ν /cm⁻¹: 3439, 2925, 2827, 1581; ¹H NMR (300 MHz, DMSO-*d*₆) (δ ppm): 8.95–8.92 (m, 2H, H_{arom.}), 8.37–8.31 (m, 2H, H_{arom.}), 8.01 (d, 1H, *J* = 9.6 Hz, H_{arom.}), 7.80–7.73 (m, 2H, H_{arom.}), 3.88 (s, 3H, CH₃), 3.83 (s, 9H, CH₃); ¹³C NMR (75 MHz, DMSO-*d*₆) (δ ppm): 157.4, 141.6, 141.5, 138.5, 135.6, 134.6, 133.9, 127.9, 126.3, 126.2, 124.2, 121.3, 118.1, 117.9, 115.6, 56.7 (3C), 30.3, elemental analysis calcd. (%) for C₁₉H₁₉N₂O₅: C 50.67, H 4.25, N 6.22; found C 50.43, H 4.53, N 6.12.

5.1.6.3. 2-(*N*-methylacetamido)-5-methyl-6-oxo-5,6-dihydro [1]benzothieno[2,3-*c*]quinoline **15**. From **3a** (0.45 g, 1.46 mmol) in DMF (25 ml), sodium hydride (0.29 g, 12.09 mmol) and methyl iodide (0.21 g, 1.45 mmol) the resulting solution was concentrated and the crude product was purified by column chromatography with dichloromethane–methanol mixture to obtain 0.02 g (4%) of ivory solid; m.p. >300 °C; IR ν /cm⁻¹: 3372, 3083, 1632, 1554; ¹H NMR (300 MHz, DMSO-*d*₆) (δ ppm): 9.01 (bs, 1H, H_{arom.}), 8.73 (s, 1H, H_{arom.}), 8.28–8.25 (m, 1H, H_{arom.}), 7.84 (d, 1H, *J* = 8.9 Hz, H_{arom.}), 7.70–7.69 (m, 3H, H_{arom.}), 3.84 (s, 3H, CH₃), 3.39 (bs, 3H, OCH₃), 1.85 (s, 3H, CH₃); ¹³C NMR (75 MHz, DMSO-*d*₆) (δ ppm): 168.6, 157.8, 142.0, 139.8 (2C), 135.6 (2C), 134.7, 128.4, 128.0, 126.5 (2C), 124.4, 122.6, 119.4, 117.7, 30.5 (2C), 22.9; elemental analysis calcd. (%) for C₁₉H₁₆N₂O₅: C 67.84, H 4.79, N 8.33; found C 68.14, H 4.64, N 8.18.

5.1.7. Preparation of 2-Amino-6-oxo-5,6-dihydro [1]benzothieno[2,3-*c*]quinoline **11**

To a solution of **3a** (0.80 g, 2.60 mmol) in methanol (55 ml) was added saturated solution of sodium hydroxide (1.52 g, 38.00 mmol). After refluxing for 24 h the solution was concentrated and the crude product was purified by column chromatography with dichloromethane–methanol mixture to obtain 0.04 g (6%) of light yellow solid; m.p. > 300 °C; IR ν /cm⁻¹: 3325, 2974, 2842, 1649, 1596, 1509; ¹H NMR (300 MHz, DMSO-*d*₆) (δ ppm): 11.95 (s, 1H, H_{quinolone}), 8.87–8.84 (m, 1H, H_{arom.}), 8.27–8.24 (m, 1H, H_{arom.}), 7.98 (d, 1H, *J* = 2.0 Hz, H_{arom.}), 7.72–7.65 (m, 2H, H_{arom.}), 7.29 (d, 1H, *J* = 8.7 Hz, H_{arom.}), 6.92 (dd, 1H, *J*₁ = 8.7 Hz, *J*₂ = 2.1 Hz, H_{arom.}), 5.25 (s, 2H, NH₂); ¹³C NMR (75 MHz, DMSO-*d*₆) (δ ppm): 157.8 (s), 141.3 (s), 139.2 (s), 138.0 (s), 134.2 (s), 134.0 (s), 133.1 (s), 127.9 (d), 126.2 (d), 125.0 (d), 124.6 (d), 122.2(d), 118.7 (d), 117.3 (d), 115.3 (s); elemental analysis calcd. (%) for C₁₅H₁₀N₂O₅: C 67.65, H 3.78, N 10.52; found C 67.95, H 3.92, N 10.37.

5.1.8. 2-Acetamido-5-[3-(*N,N*-dimethylamino)propyl]-6-oxo-5,6-dihydro [1]benzothieno[2,3-*c*]quinoline **13**

To a cold solution of **3a** (0.30 g, 0.97 mmol) in anhydrous DMF (18 ml), sodium hydride (0.19 g, 8.09 mmol) as 60–65% oil dispersion was added in two portions. After stirring for 15 min a

solution of 3-(dimethylamino)propyl chloride hydrochloride (0.40 g, 2.53 mmol) in DMF (18 ml) was added to the solution and the reaction mixture was stirred for 2 h at 0–5 °C and 24 h at room temperature. The solid was separated by filtration and the solvent was removed under reduced pressure. The crude product was recrystallized from ethanol to obtain 0.85 g (22%) of light yellow solid; m.p. 244–246 °C; IR ν/cm^{-1} : 3325, 2949, 2768, 1688, 1619, 1583; ^1H NMR (600 MHz, DMSO- d_6) (δ ppm): 10.32 (s, 1H, H_{amide}), 9.25 (s, 1H, $\text{H}_{\text{arom.}}$), 8.80–8.78 (m, 1H, $\text{H}_{\text{arom.}}$), 8.29–8.27 (m, 1H, $\text{H}_{\text{arom.}}$), 7.89 (d, 1H, $J = 9.2$ Hz, $\text{H}_{\text{arom.}}$), 7.79 (d, 1H, $J = 9.4$ Hz, $\text{H}_{\text{arom.}}$), 7.74–7.70 (m, 2H, $\text{H}_{\text{arom.}}$), 4.42 (t, 2H, $J = 7.4$ Hz, CH_2), 2.38 (t, 2H, $J = 6.7$ Hz, CH_2), 2.18 (s, 6H, CH_3), 2.16 (s, 3H, CH_3), 1.89–1.80 (m, 2H, CH_2); ^{13}C NMR (150 MHz, DMSO- d_6) (δ ppm): 168.6, 156.9, 141.6, 135.2, 134.6, 134.4, 133.1, 132.2, 127.4, 125.9, 125.0, 124.3, 120.3, 118.5, 116.2, 113.1, 56.3, 45.1, 40.6, 25.5, 24.1; elemental analysis calcd. (%) for $\text{C}_{22}\text{H}_{23}\text{N}_3\text{O}_2\text{S}$: C 67.15, H 5.98, N 10.68; found C 67.35, H 5.63, N 10.78.

5.1.9. General method for the synthesis of and 6-oxo-5,6-dihydro [1]benzothieno[2,3-*c*]quinoline hydrochlorides (10,12,14)

A stirred suspension of compounds **9a**, **11** and **13** in absolute ethanol was saturated with HCl(g). After 20 h of stirring resulting product was filtered off and washed with diethyl ether to obtain 6-oxo-5,6-dihydro [1]benzothieno[2,3-*c*]quinoline hydrochlorides.

5.1.9.1. 2-(*N,N'*-dimethylamino)-5-methyl-6-oxo-5,6-dihydro [1]benzothieno[2,3-*c*]quinoline hydrochloride **10**. Compound **10** was prepared using above described method from **9a** (0.04 g, 0.14 mmol) in absolute ethanol (10 ml) to obtain 0.03 g (67%) of brown solid; m.p. >300 °C; IR ν/cm^{-1} : 3400, 2548, 2445, 1633, 1587; ^1H NMR (300 MHz, DMSO- d_6) (δ ppm): 9.04–8.92 (m, 2H, $\text{H}_{\text{arom.}}$), 8.19 (d, 1H, $J = 8.6$ Hz, $\text{H}_{\text{arom.}}$), 8.00 (bs, 1H, $\text{H}_{\text{arom.}}$), 7.80 (d, 1H, $J = 9.2$ Hz, $\text{H}_{\text{arom.}}$), 7.76–7.59 (m, 2H, $\text{H}_{\text{arom.}}$), 3.88 (bs, 1H, NH^+), 3.74 (s, 3H, CH_3), 3.22 (s, 6H, CH_3); ^{13}C NMR (75 MHz, DMSO- d_6) (δ ppm): 157.5, 141.8 (2C), 138.8, 135.2, 134.3, 133.3, 128.0, 126.4 (2C), 126.2, 124.5 (2C), 118.6, 118.3, 45.4 (2C), 30.4; elemental analysis calcd. (%) for $\text{C}_{18}\text{H}_{17}\text{ClN}_2\text{OS}$: C 62.69, H 4.97, N 8.12; found C 62.89, H 4.82, N 8.24.

5.1.9.2. 2-Amino-6-okso-5,6-dihidro [1]benzothieno[2,3-*c*]quinoline hydrochloride **12**. Compound **12** was prepared using above described method from **11** (0.08 g, 0.30 mmol) in absolute ethanol (15 ml) to obtain 0.05 g (53%) of light brown solid; m.p. >300 °C; IR ν/cm^{-1} : 3331, 2964, 2858, 1652; ^1H NMR (600 MHz, DMSO- d_6) (δ ppm): 12.41 (s, 1H, $\text{H}_{\text{quinolone}}$), 10.17 (bs, 3H, NH_3^+) 8.90–8.88 (m, 2H, $\text{H}_{\text{arom.}}$), 8.32–8.29 (m, 1H, $\text{H}_{\text{arom.}}$), 7.73–7.71 (m, 2H, $\text{H}_{\text{arom.}}$), 7.63 (d, 1H, $J = 8.7$ Hz, $\text{H}_{\text{arom.}}$), 7.52 (dd, 1H, $J_1 = 8.7$ Hz, $J_2 = 2.0$ Hz, $\text{H}_{\text{arom.}}$); ^{13}C NMR (75 MHz, DMSO- d_6) (δ ppm): 158.6 (s), 140.8 (s), 139.3 (s), 137.6 (s), 134.7 (s), 133.9 (s), 131.2 (s), 128.3 (d), 126.9 (d), 125.3 (d), 124.0 (d), 121.8 (d), 119.2 (d), 117.1 (d), 116.0 (s); elemental analysis calcd. (%) for $\text{C}_{15}\text{H}_{11}\text{ClN}_2\text{OS}$: C 59.50, H 3.66, N 9.25; found C 59.15, H 3.81, N 9.45.

5.1.9.3. 2-Acetamido-5-[3-(*N,N'*-dimethylamino)propyl]-6-oxo-5,6-dihidro [1]benzothieno[2,3-*c*]quinoline hydrochloride **14**. Compound **14** was prepared using above described method from **13** (0.06 g, 0.15 mmol) in absolute ethanol (10 ml) to obtain 0.06 g (94%) of white solid; m.p. 222–224 °C; IR ν/cm^{-1} : 3373, 3066, 2660, 1628, 1587; ^1H NMR (300 MHz, DMSO- d_6) (δ ppm): 10.56 (bs, 2H, H_{amide} , NH^+), 9.12 (s, 1H, $\text{H}_{\text{arom.}}$), 8.77–8.75 (m, 1H, $\text{H}_{\text{arom.}}$), 8.21–8.18 (m, 1H, $\text{H}_{\text{arom.}}$), 7.92 (d, 1H, $J = 8.5$ Hz, $\text{H}_{\text{arom.}}$), 7.76 (d, 1H, $J = 9.2$ Hz, $\text{H}_{\text{arom.}}$), 7.66–7.63 (m, 2H, $\text{H}_{\text{arom.}}$), 4.44 (bs, 2H, CH_2), 3.25–3.18 (m, 2H, CH_2), 2.73 (s, 3H, CH_3), 2.48 (bs, 2H, CH_2), 2.14 (s, 6H, CH_3); ^{13}C NMR (75 MHz, DMSO- d_6) (δ ppm): 169.2, 157.6, 142.1, 135.5, 135.4, 135.2, 133.2, 132.3, 128.0, 126.4, 125.7, 124.6, 120.7,

119.0, 116.7, 113.5, 54.5, 42.5 (2C), 39.2, 24.6, 23.2; elemental analysis calcd. (%) for $\text{C}_{22}\text{H}_{24}\text{ClN}_3\text{O}_2\text{S}$: C 61.46, H 5.63, N 9.77; found C 61.54, H 5.51, N 10.04.

5.2. Antiproliferative evaluation assay

The experiments were carried out on three human cell lines, which are derived from three cancer types. The following cell lines were used: HCT 116 (colon carcinoma), H 460 (lung carcinoma) and MCF-7 (breast carcinoma). The cells were cultured as monolayers and maintained in Dulbecco's modified Eagle medium (DMEM) supplemented with 10% fetal bovine serum (FBS), 2 mM L-glutamine, 100 U/ml penicillin and 100 $\mu\text{g}/\text{ml}$ streptomycin in a humidified atmosphere with 5% CO_2 at 37 °C. The cell lines were inoculated onto a series of standard 96-well microtiter plates on day 0, at 3×10^4 cells/mL (HCT 116, H 460) to 5×10^4 cells/mL (MCF-7), depending on the doubling times of a specific cell line. After 24 h, cells were treated with indicated compounds and concentrations where highest DMSO concentration at <1%. Following a 72 h incubation, an MTT assay (Sigma) was performed per standard protocol, as described previously [15–18]. The absorbance (*A*) of the microtiter plate was measured on a microplate reader at 570 nm where absorbance is directly proportional to the number of living, metabolically active cells. Each treatment was performed in technical quadruplicates, with at least 2 biological replicates. The results are expressed as IC_{50} , which is the concentration necessary for 50% of inhibition. The IC_{50} values for each compound are calculated from concentration–response curves using linear regression analysis by fitting the test concentrations that give percentage of growth (PG) values above and below the reference value (*i.e.* 50%).

5.3. Computational analysis

Measured anticancer activity of the presented compounds against MCF-7 (breast carcinoma), HCT116 (colon carcinoma) and H460 (lung carcinoma) were used to build 3D-derived QSAR models. Negative logarithmic value of the concentration that causes 50% growth inhibition of the cell lines (pIC_{50}) was used as measure of compound's anticancer activity in the 3D-derived QSAR models. For the poorly active compounds whose IC_{50} values were not explicitly measured, but just estimated as ≥ 100 , pIC_{50} was set to 3.301. Volsurf + program [19] was applied for generation of molecular descriptors for each compound (for detailed description of all 128 VolSurf + descriptors see the VolSurf + manual [27]). Grid spacing was set to 0.5 Å and the following probes were used: H₂O (the water molecule), O (sp^2 carbonyl oxygen atom), N1 (neutral NH group (*e.g.* amide)) and DRY (the hydrophobic probe).

For each cell line, 3D-derived QSAR models were derived using either autoscaled variables (models labeled as A) or raw data (models labeled as B). Partial Least Square (PLS) analysis was applied to find the relationship between the 3D structure-based molecular descriptors and measured antitumor activity. In order to identify the descriptors with the highest (positive or negative) impact on biological activity of the compounds, PLS coefficients of the 3D-derived QSAR models were analyzed using the procedure described in previous work [18,24,25]. In case of the models derived using autoscaling procedure, the influence of each descriptor to the QSAR model was estimated from its PLS coefficient. In case of models derived using raw data (**1B** and **2B**), product between average value of the descriptor (calculated for the dataset used to build the model) and its associated PLS coefficient was calculated for each descriptor.

Principal component analysis (PCA) was performed in order to determine distribution of the compounds in the space of the molecular descriptors (PCA scores plot) and to find contribution of

each descriptor to the first two principal components (PCA loadings plot). Usefulness of PCA in 3D-derived QSAR analysis has already been proved in several cases [18,25,28,29].

5.4. DNA binding properties and topoisomerase assays

5.4.1. Spectroscopic analyses of DNA binding

CT-DNA (Sigma Aldrich, France) was dissolved in water and dialyzed overnight prior to use. The analyzed compounds were prepared as 10 mM stock solutions in DMSO, aliquoted and stored at $-20\text{ }^{\circ}\text{C}$ and then freshly diluted in the appropriate aqueous buffer.

For UV/visible spectroscopy, tested compounds (20 μM) were diluted in 1 mL of BPE buffer (6 mM Na_2HPO_4 , 2 mM NaH_2PO_4 , 1 mM EDTA, pH 7.1) in the presence or absence of increasing concentrations of CT-DNA (from 10 to 100 μM with 10 μM steps and then from 100 to 200 μM with steps of 20 μM of base pairs). The UV/Visible spectra were recorded from 230 nm to 530 nm in a quartz cuvette of 10 mm pathlength using an Uvikon XL spectrophotometer and referenced against a cuvette containing DNA at identical concentration.

For melting temperature studies, the absorbency of DNA was measured at 260 nm in quartz cells using an Uvikon 943 spectrophotometer thermostated with a Neslab RTE111 cryostat every min over a range of 20–100 $^{\circ}\text{C}$ with an increment of 1 $^{\circ}\text{C}$ per min. The T_m values were obtained from the midpoint of the hyperchromic transition obtained from first-derivative plots. The variation of melting temperature (ΔT_m) were measured by subtracting the melting temperature measurement of 20 μM of CT-DNA or poly(-dAdT)₂ incubated alone (control T_m) to that obtained with DNA incubated with increasing concentrations of the various tested compounds ($R = \text{drug/base pair ratio from 0.25 to 1}$) in 1 mL BPE buffer ($\Delta T_m \text{ values} = T_{m[\text{Drug} + \text{DNA}]} - T_{m[\text{DNA alone}]}$).

For circular dichroism, the various drugs (50 μM) were incubated with or without (control) a fixed or increasing concentrations of CT-DNA (from 0.1 to 100 μM) in BPE. The CD spectra were collected in a quartz cell of 10 mm path length from 480 to 230 nm using a J-810 Jasco spectropolarimeter at a controlled temperature of 20 $^{\circ}\text{C}$ fixed by a PTC-424S/L peltier type cell changer (Jasco) as described previously [30].

5.4.2. DNase I footprinting

DNase I footprinting experiments were conducted essentially as previously described [31]. After an exposition of the gels to storage screen for the appropriated delay at room temperature, the results were collected using a Molecular Dynamics STORM 860.

5.4.3. Topoisomerase-mediated DNA relaxation and topoisomerase II cleavage assay

Topoisomerase I-mediated DNA relaxation experiment was performed as previously described [26] using supercoiled pUC19 plasmid DNA and human topoisomerase I (Topogen, USA). The reactions were stopped upon addition of SDS and proteinase K prior to gel electrophoresis on a 1% agarose gel for 2 h at 120 V in TBE buffer. Gels were then stained in a bath containing ethidium bromide before being washed and photographed under UV light. Topoisomerase II DNA cleavage assays were performed essentially as described with etoposide as a positive control for Topo II poisoning effect.

Acknowledgments

We greatly appreciate the financial support of the Croatian Ministry of Science Education and Sports (projects 125-0982464-1356, 098-098-1192344-2860, 098-098-2464-2514) and the

bilateral Hubert Curien partnership between Croatian and French institutions (Cogito program) as the Egide project N $^{\circ}$ 24765PH. M.-H.D.-C. thanks the Association pour la Recherche sur le Cancer (ARC) Ligue Nationale Contre le Cancer (Comité du Pas-de-Calais, Septentrion), the Fonds Européen de Développement Régional (FEDER, European Community) and the Région Nord/Pas-de-Calais for grants (M.-H.D.-C.), the Institut pour la Recherche sur le Cancer de Lille (IRCL) for Ph.D and post-doctoral fellowships (R.N.) and technicien expertise (S.D.).

Appendix A. Supplementary material

Supplementary material related to this article can be found at <http://dx.doi.org/10.1016/j.ejmech.2013.11.010>.

References

- [1] P. Diana, A. Martorana, P. Barraja, A. Montalbano, G. Dattolo, G. Cirrincione, F. Dall'Acqua, A. Salvador, D. Vedaldi, G. Basso, G. Viola, Isoindolo[2,1-*g*]quinoxaline derivatives, novel potent antitumor agents with dual inhibition of tubulin polymerization and topoisomerase I, *J. Med. Chem.* 51 (2008) 2387–2399.
- [2] L. Wilson, M.A. Jordan, Microtubule dynamics: taking aim at a moving target, *Chem. Biol.* 2 (1995) 569–573.
- [3] I.V. Magedov, M. Manpadi, M.A. Ogasawara, A.S. Dhawan, S. Rogelj, S. Van Slambrouck, W.F. Steelant, N.M. Evdokimov, P.Y. Ugliński, E.M. Elias, E.J. Knee, P. Tongwa, M.Y. Antipin, A. Kornienko, Structural simplification of bioactive natural products with multicomponent synthesis. 2. Antiproliferative and antitubulin activities of pyrano[3,2-*c*]pyridones and pyrano[3,2-*c*]quinolones, *J. Med. Chem.* 51 (2008) 2561–2570.
- [4] A.A. Sagardoy, M.J. Gil, R. Villar, M.J. Vinas, A. Arrazola, I. Encio, V. Martinez-Merino, Benzo[*b*]thiophene-6-carboxamide 1,1-dioxides: inhibitors of human cancer cell growth at nanomolar concentrations, *Bioorg. Med. Chem.* 18 (2010) 5701–5707.
- [5] B. Letafat, S. Emami, N. Mohammadhosseini, M.A. Faramarzi, N. Samadi, A. Shafiee, A. Foroumadi, Synthesis and antibacterial activity of new N-[2-(thiophen-3-yl)ethyl]piperazinyl Quinolones, *Chem. Pharm. Bull.* 55 (2007) 894–898.
- [6] S.W. Wang, S.L. Pan, Y.C. Huang, J.H. Guh, P.C. Chiang, D.Y. Huang, S.C. Kuo, K.H. Lee, C.M. Teng, CHM-1, a novel synthetic quinolone with potent and selective antimetabolic antitumor activity against human hepatocellular carcinoma in vitro and in vivo, *Mol. Cancer Ther.* 7 (2008) 350–360.
- [7] H. Hoang, D.V. LaBarbera, K.A. Mohammed, C.M. Ireland, E.B. Skibo, Synthesis and biological evaluation of imidazoquinolones, imidazole analogues of pyrrolo- iminoquinone marine natural products, *J. Med. Chem.* 50 (2007) 4561–4571.
- [8] R. Romagnoli, P.G. Baraldi, M.D. Carrion, O. Cruz-Lopez, M. Tolomeo, S. Grimaudo, A. Di Cristina, M.R. Pipitone, J. Balzarini, A. Brancale, E. Hamel, Substituted 2-(3',4',5'- trimethoxybenzoyl)-benzo[*b*]thiophene derivatives as potent tubulin polymerization inhibitors, *Bioorg. Med. Chem.* 18 (2010) 5114–5122.
- [9] M.J.R.P. Queiroz, R.C. Calhelha, L.A. Vale-Silva, E. Pinto, M.S.J. Nascimento, Synthesis of novel 3-(aryl)benzothieno[2,3-*c*]pyran-1-ones from Sonogashira products and intramolecular cyclization: antitumoral activity evaluation, *Eur. J. Med. Chem.* 44 (2009) 1893–1899.
- [10] A.P. Ferreira, J.L.F. da Silva, M.P. Duarte, M.F.M. da Piedade, M.P. Robalo, S.G. Harjivan, C. Marzano, V. Gandin, M.M. Marques, Synthesis and characterization of new organometallic Benzo[*b*]thiophene derivatives with potential antitumor properties, *Organometallics* 28 (2009) 5412–5423.
- [11] C. Mésangeau, M. Fraise, P. Delagrangue, D.H. Caignard, J.A. Boutin, P. Berthelot, S. Yous, Preparation and pharmacological evaluation of a novel series of 2-(phenylthio)benzo[*b*]thiophenes as selective MT₂ receptor ligands, *Eur. J. Med. Chem.* 46 (2011) 1835–1840.
- [12] S. Dadiboyena, Recent advances in the synthesis of raloxifene: a selective estrogen receptor modulator, *Eur. J. Med. Chem.* 51 (2012) 17–34.
- [13] J. Dogan Koruznjak, N. Slade, B. Zamola, K. Pavelić, G. Karminski-Zamola, Synthesis, photochemical synthesis and antitumor evaluation of novel derivatives of thieno[3',2': 4, 5] thieno[2,3-*c*]quinolones, *Chem. Pharm. Bull.* 50 (2002) 656–660.
- [14] J. Dogan Koruznjak, M. Grdiša, N. Slade, B. Zamola, K. Pavelić, G. Karminski-Zamola, Novel derivatives of benzo[*b*]thieno[2,3-*c*]quinolones: synthesis, photochemical synthesis and antitumor evaluation, *J. Med. Chem.* 45 (2003) 4516–4524.
- [15] I. Jarak, M. Kralj, L. Šuman, G. Pavlović, J. Dogan, I. Piantanida, M. Žinić, K. Pavelić, G. Karminski-Zamola, Novel cyano- and N-isopropylamido-substituted derivatives of Benzo[*b*]thiophene- 2-carboxanilides and benzo[*b*]thieno[2,3-*c*]quinolones: synthesis, photochemical synthesis, crystal structure determination and antitumor evaluation. Part 2, *J. Med. Chem.* 48 (2005) 2346–2360.

- [16] I. Jarak, M. Kralj, I. Piantanida, L. Šuman, M. Žinić, K. Pavelić, G. Karminski-Zamola, Novel cyano- and amidino-substituted derivatives of thieno[2,3-*b*]- and thieno[3,2-*b*]thiophene-2-carboxanilides and Thieno[3',2':4,5]thieno- and Thieno[2',3':4,5]thieno[2,3-*c*]quinolones: synthesis, photochemical synthesis, DNA binding and antitumor evaluation, *Bioorg. Med. Chem.* 14 (2006) 2859–2868.
- [17] K. Ester, M. Hranjec, I. Piantanida, I. Čaleta, I. Jarak, K. Pavelić, M. Kralj, G. Karminski-Zamola, Novel derivatives of Pyridylbenzo[*b*]thiophene-2-carboxamides and benzo[*b*]thieno[2,3-*c*]naphthyridin-2-ones: minor structural variations Provoke major differences of antitumor action mechanisms, *J. Med. Chem.* 52 (2009) 2482–2492.
- [18] M. Aleksić, B. Bertoša, R. Nhili, L. Uzelac, I. Jarak, S. Depauw, M.H. David Cordonnier, M. Kralj, S. Tomić, G. Karminski-Zamola, Novel substituted benzothiofene and thienothiofene carboxanilides and quinolones: synthesis, photochemical synthesis, DNA binding properties, antitumor evaluation and 3D-derived QSAR analysis, *J. Med. Chem.* 55 (2012) 5044–5060.
- [19] G. Cruciani, P. Crivori, P.-A. Carrupt, B. Testa, Molecular fields in quantitative structure-permeation relationships: the VolSurf approach, *J. Mol. Struct. Theochem.* 503 (2000) 17–30.
- [20] C.G. Fortuna, V. Barresi, G. Berellini, G. Musumarra, Design and synthesis of trans 2-(furan-2-yl)vinyl heteroaromatic iodides with antitumour activity, *Bioorg. Med. Chem.* 16 (2008) 4150–4159.
- [21] X.-M. Zhuang, J.-H. Xiao, J.-T. Li, Z.-Q. Zhang, J.-X. Ruan, A simplified model to predict *P*-glycoprotein interacting drugs from 3D molecular interaction field, *Int. J. Pharm.* 309 (2006) 109–114.
- [22] I. Čaleta, M. Kralj, M. Marjanović, B. Bertoša, S. Tomić, G. Pavlović, K. Pavelić, G. Karminski-Zamola, Novel cyano- and amidinobenzothiazole derivatives: synthesis, antitumor evaluation, and X-ray and quantitative structure–activity relationship (QSAR) analysis, *J. Med. Chem.* 52 (2009) 1744–1756.
- [23] B. Bertoša, B. Kojić-Prodić, M. Ramek, S. Piperaki, A. Tsantili-Kakoulidou, R. Wade, S. Tomić, A new approach to predict the biological activity of molecules based on similarity of their interaction fields and the log P and log D values: application to auxins, *J. Chem. Inf. Model* 43 (2003) 1532–1541.
- [24] I. Vujašinić, A. Paravić-Radičević, K. Mlinarić-Majerski, K. Brajša, B. Bertoša, Synthesis and biological validation of novel pyrazole derivatives with anticancer activity guided by 3D-QSAR analysis, *Bioorg. Med. Chem.* 20 (2012) 2101–2110.
- [25] B. Bertoša, M. Aleksić, G. Karminski-Zamola, S. Tomić, QSAR analysis of antitumor active amides and quinolones from thiophene series, *Int. J. Pharm.* 394 (2010) 106–114.
- [26] P. Peixoto, C. Bailly, M.-H. David-Cordonnier, Topoisomerase I-mediated DNA relaxation as a tool to study intercalation of small molecules into supercoiled DNA, *Methods Mol. Biol.* 613 (2010) 235–256.
- [27] G. Cruciani, M. Pastor, W. Guba, VolSurf: a new tool for pharmacokinetic optimization of lead compounds, *Eur. J. Pharm. Sci.* 11 (2000) S29–S39.
- [28] S. Tomić, B. Bertoša, B. Kojić-Prodić, I. Kolosvary, Stereoselectivity of *Burkholderia cepacia* lipase towards secondary alcohols: molecular modelling and 3D QSAR approach, *Tetrahedron: Asymmetry* 15 (2004) 1163–1172.
- [29] S. Tomić, B. Bertoša, T. Wang, R.C. Wade, COMBINE analysis of the specificity of binding of Ras proteins to their effectors, *Proteins Struct. Funct. Bioinform.* 67 (2) (2007) 435–447.
- [30] T. Lemster, U. Pindur, S. Depauw, G. Lenglet, C. Dassi, M.-H. David-Cordonnier, Photochemical electrocycloisolation of 3-vinylindoles to pyrido[2,3-*a*]-, pyrido[4,3-*a*]- and thieno[2,3-*a*]-carbazoles: design, synthesis, DNA-binding and antitumor cell cytotoxicity, *Eur. J. Med. Chem.* 44 (2009) 3235–3252.
- [31] P. Peixoto, Y. Liu, S. Depauw, M.-P. Hildebrand, D.W. Boykin, C. Bailly, W.D. Wilson, M.-H. David-Cordonnier, Direct inhibition of the DNA binding activity of POU transcription factors Pit-1 and Brn-3 by selective binding of a phenyl-furan-benzimidazole dication, *Nucleic Acids Res.* 36 (2008) 3341–3353.